FACTORS INFLUENCING THE ACCURACY OF ROCKETS

Thesis by

Leon Blitzer

In Partial Fulfillment of the Requirements for the

Degree of Doctor of Philosophy

California Institute of Technology

Pasadena, California

1943

ABSTRACT

The inaccuracy of rockets arises primarily from the failure of the axis of the jet to pass through the center of mass of the projectile. This causes the rocket to rotate, during burning, about a transverse axis through the center of mass, with the result that the direction of thrust of the motor is altered from its initial direction as determined by the projector.

A theoretical analysis of the forces acting on a rocket during its accelerating period leads to the following conclusions concerning the effects of malalignment, burning time, fin size and projector length on the accuracy of rockets with velocities less than 800 ft/sec:

(i) The deflection of the rocket is directly proportional to the malalignment of the jet.

(ii) For projector lengths less than one-fifth the burning distance the deflection of a rocket increases rapidly with the burning time until the burning time equals the period of oscillation of the projectile in free flight, or until the burning distance equals half the yaw oscillation distance in free flight. Further increases in burning time produce no significant change in the deflection.

(iii) In the same range of projector lengths, increasing the fin size from that required to make the projectile barely stable in free flight to that which reduces the period of oscillation to the burning time diminishes the deflection by a factor of about 0.7. Still further reduction in the period by increasing the fin size decreases the deflection roughly proportionally to the period attained.

(iv) When the ratio of projector length to burning distance is in the range between 0.01 and 0.50, the deflection decreases roughly linearly with the logarithm of this ratio.

On the basis of certain simplifying assumptions, formulas are derived for the effect of wind on the motion of rockets with velocities less than 800 ft/sec. The effect of the wind is to deflect the UP into the wind during burning and down wind after burning, the relative effects of each depending mainly upon the burning time. The formulas developed apply to the mean deflection for a given set of firings of a sufficient number of rounds so that malalignment and other such random effects average out.

Preface

In this thesis, the theory of non-rotating rockets is studied, quite apart from any considerations regarding particular applications of rockets. Its immediate application, of course, is in the development of rockets for purposes of the successful prosecution of the war; but it is hoped that the results herein attained will in time find application to rockets in scientific and peace time pursuits.

The references to the literature are quite meager, since the developments in rocket ballistics are very recent, and there is practically no published material on the subject. Most of the material contained herein has already appeared in the form of CIT and NDRC reports; for example, Chapter III is merely an amplification of "Effects of Burning Time, Fin Size and Projector Length on the Accuracy of Rockets" by I. S. Bowen, L. Davis, Jr. and Leon Blitzer.

I wish to thank Prof. I. S. Bowen who suggested most of the problems and under whose encouraging supervision this work was done. To Dr. Leverett Davis, Jr., I am grateful for considerable practical help in dealing with the problems, to which specific acknowledgment is frequently made in the text. I am also indebted to the many members of the research staff of the NDRC project at Kellogg Laboratory, especially Dr. O. C. Wilson, Mr. S. Rubin and Dr. G. Kron of the Accuracy Committee, who aided with the experimental data.

Table of Contents

Symbols Frequently Used

(The use of certain symbols for more than one quantity is sometimes unavoidable. However, there is little chance for ambiguity, as the text generally makes the meaning of the symbols clear.)

c	Deceleration coefficient of the rocket
F	Force on the rocket ($F = mG$)
G	Linear acceleration of the rocket during burning
I	Moment of inertia of the rocket about a transverse axis through the center of mass ($I = mk^2$)
k	Radius of gyration of the rocket ($k^2 = I/m$)
K	Moment coefficient of the fins; the aerodynamic restoring torque is $-K v^2$.
$L(t)$	Malalignment of the jet; that is, the distance between the axis of thrust and the center of mass
L_o	Malalignment of the jet in the case of constant malalignment
m	Mass of the rocket
p	Effective projector length; that is, the distance the rocket moves before the constraint of the projector is removed
s	Distance along the trajectory
t	(generally) Time from start of burning
t_b	Time at which burning ceases
t_p	Time when rocket leaves the projector
T	Period of yaw oscillation (for the velocity v_b)
T_1	Total flight time of the rocket
v	Velocity of the rocket (During burning, $v = Gt$.)
v_b	Velocity of the rocket at the end of burning
$\bar{v}_a$	Vector velocity of the rocket relative to the moving air (wind)

$\bar{w}$ Vector velocity of the wind

$W_\perp$ Cross-range component of the wind velocity $\bar{w}$

$W_{//}$ Down-range component of the wind velocity $\bar{w}$

x Horizontal distance of rocket travel

X Range

y Vertical height of the rocket

z In the D-B theory, z is the dimensionless parameter $2c\alpha x$

z In the theory of yaw and deflection, z is the dimensionless quantity $\sqrt{2\pi G/\sigma}\, t$

α Average of $1/\cos\theta$ in the D-B theory

β Lateral deflection of rocket on range

β_0 Mean lateral up-wind deflection produced by the wind during the burning period

β_1 Mean lateral down-wind deflection produced by the wind after the burning period

δ_c Yaw of the rocket in the plane of yaw ($\delta_c = \phi_c - \theta_c$)

μ Damping coefficient; damping moment is $-\mu\dot{\phi}_c$

ϕ_c Angle between the axis of the rocket and the initial direction on the projector in the plane of yaw

θ_c Angle between trajectory and initial direction (θ_c is the deflection in the plane of yaw.)

θ_0 Quadrant angle of the projector

σ Distance traversed by the rocket in free flight while the yaw oscillates through one full cycle ($\sigma = v_b T$)

I. Artillery Projectiles and Rockets

A. Introduction:

It was known to the ancients that hot gases (especially steam) were capable of expansion and doing work. Archimedes[1)] supposedly had a gun operated by high-pressure steam instead of by powder. The principle of jet propulsion must have been known to Hero of Alexandria[1)] (120 B.C.) who built the first prototype of modern jet propulsion devices. The rocket, too, depends for its action on the principle of jet propulsion, or, in other words, the principle of conservation of momentum; for the release of hot gases at extremely high velocities as the products of combustion in the rocket motor result in the rocket taking up an equal and opposite momentum and thus being propelled.

Among the types of rockets which one may encounter are the following:

1. War Rockets.- For a long time military engineers have sought to develop rockets as combat weapons; but very little progress was made until Congreve's work[2)] in England early in the 19th century. His rockets were very much like the present-day ones and were used on sea (His boats were fitted for firing salvos of rockets.) and on land during the Napoleonic wars. However, the use of such rockets ended with the development of high-precision gunnery toward the latter part of the 19th century.

2. Signal Rockets.- These are rockets containing flares for signalling purposes.

3. Life-saving Rockets.- These are line-carrying rockets for establishing breeches-buoys from ship to shore or from ship to ship.

4. Sounding Rockets.- These are for meteorological purposes to travel into the upper atmosphere to obtain data as to its composition and condition.

5. Auxiliary Propulsive Rockets for Airplanes.- These are rockets attached to planes for aiding them in quick take-offs from small landing fields.

The types of rockets mentioned in this paper are all war rockets. However, the theory developed herein should be quite applicable to all similar rockets.

Note: It is common practice to refer to finned rockets which do not rotate as UP's (unrotating projectiles), and since we are concerned only with such projectiles we shall use the terms rocket and UP interchangeably.

B. Characteristics of Artillery Projectiles and Rockets:

Since the introduction of gun-powder in Europe the common form of hurling large missiles has been from guns and cannon; that is, the explosion of a charge of powder to the rear of the shell releases hot gases whose pressure forces the projectile out of the gun barrel at high speed. Because of the conservation of momentum, as the fast-moving shell leaves the barrel, the gun suffers a "kick" or recoil, the magnitude of which depends upon the mass and velocity of the projectile. To reduce this recoil motion of the gun is not an easy problem; in addition to having heavy mounts, cannon are generally equipped with complicated recoil mechanisms. With the invention of the rifled bore, streamlined elongated projectiles replaced the former cannon-balls, and the accuracy of artillery fire was very greatly improved.

Once the projectile leaves the gun barrel propulsion ceases, the remaining action being that of gravity and aerodynamic forces. The spin imparted to the shell by the rifling serves to introduce gyroscopic forces which prevent the body from tumbling, as it would normally do because of

the aerodynamic destabilizing moment (Sec. C, below). The very great advantage of standard artillery over rockets is its unequalled great accuracy.

Compared to the ordinary gun, the rocket projector is simplicity itself; for, the backward momentum being taken up by the burnt gases which expand into the atmosphere, there is no need for a heavy gun or mount or recoil mechanism. All that is necessary is a tube or a set of rails or some similar guide for the rocket during the first few feet of its motion. However, even after the rocket leaves the projector it continues to be accelerated forward by the jet-propulsive action, often for a considerable distance; and it is during this period that practically all of the deviations in range and deflection are introduced. In order that the UP be stable in flight (cf. Sec. C, below) fins are attached at its rear. Because of the unguided burning period off the rails the accuracy of rocket fire is so poor compared to standard artillery fire that more approximate methods of treating the ballistics problem are justified on this account.

C. The Force System Acting on a Yawing Projectile:

Consider a projectile moving through the air (Fig. 1) with its axis making an angle δ (angle of yaw) with the direction of motion. It will be acted upon by gravity and by an air force, F, depending upon the characteristics of the projectile and of the air and also upon the velocity and yaw. The gravitational force being constant in all practical cases, it is not necessary to consider it further for the moment. From mechanics we know that the whole of the forces acting on a rigid body are always reducible to a single force, acting at a given point and a couple. In a projectile this true couple is negligible;[3] while the point of application

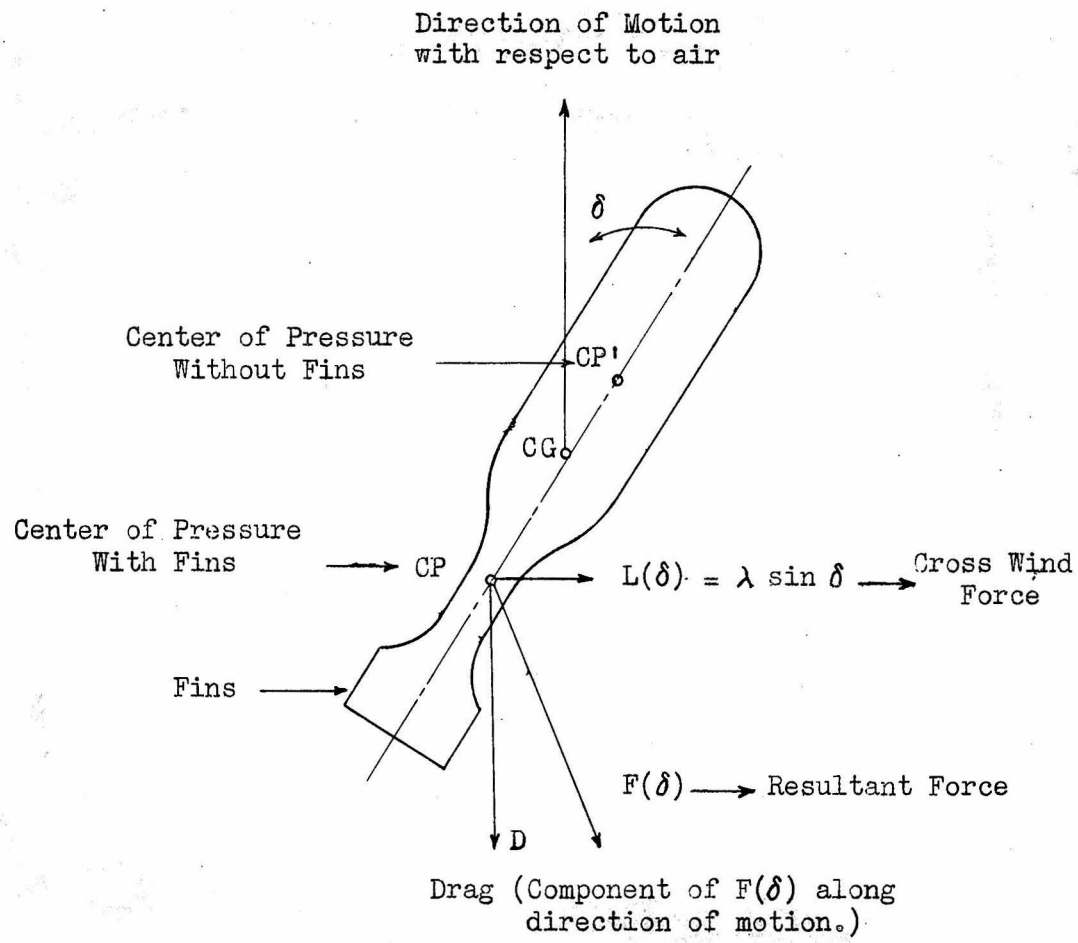

Fig. 1

of the total force on the body under a fixed angle of yaw is called the center of pressure (C. P.). In general, an artillery projectile has its C. P. ahead of its center of gravity (C. G.); consequently the air forces tend to cause such a projectile to tumble, because of the overturning moment of the force F about the C. G. The existence of this destabilizing moment is an intrinsic property of elongated bodies moving end-on.[4] For stable flight, therefore, a projectile either must be given a fast spin about its longitudinal axis (for gyroscopic effect), or else it must have fins located at the tail (as in airplane bombs and rockets) to bring the C. P. back of the C. G., so that the aerodynamic torque is a restoring

one instead of a destabilizing one. In addition, since the yaw varies with time, there exists a damping couple because of the air resistance to angular motion.

The component of the total force, F, along the direction of motion is called the drag or head resistance, D; while the component perpendicular to the direction of motion is called the cross-wind force, L. By dimensional reasoning one can easily arrive at the following expressions for the drag, cross-wind force and the moment M of F about the C. G.

$$D = K_D \rho d^2 v^2 \qquad (1)$$

$$L = \lambda \sin \delta = K_L \rho d^2 v^2 \sin \delta \qquad (2)$$

$$M = K_M \rho d^3 v^2 \sin \delta \qquad (3)$$

where ρ is the density of the air; d is some characteristic linear dimension of the projectile; and K_D, K_L and K_M are dimensionless coefficients which are functions of $\rho vd/\sigma$ (Reynolds number), v/a (Mach number) and δ; while σ and a are the coefficient of viscosity of the air and the velocity of sound in the air, respectively. Since L and M vanish as $\delta \to o$, the factor $\sin\delta$ has been included in equations (2) and (3).

Little is known about the dependence of the K's on Reynolds number; but various determinations of the variations of the coefficients with v/a have been made in this country[3] (at the Aberdeen Proving Gounds) and elsewhere (e.g. the experimental studies conducted by the Gâvre Commission in France). It has been found that no simple function represents the dependence of K_D, K_L or K_M on velocity. However, from the lowest velocities used in artillery up to about v/a = 0.8 the K's are approximately constant; while as v/a increases the coefficients increase extremely rapidly, approaching a maximum at roughly v/a = 1 and then decreasing somewhat. In general the forms of the curves are different for different projectile shapes.

Another way of stating the above is that up to a velocity of about 800 ft/sec the forces on the projectile vary as the square of the velocity.

As for the dependence of the coefficients on the yaw, experiments indicate[5] that K_D is a linear function of δ^2. ($K_D = C_1 + C_2 \delta^2$); while, for small yaws, K_L and K_M are approximately independent of δ.

II. Trajectories of Low-Velocity Projectiles

A. Exterior Ballistics:

The object of this section is to deal with some simple problems of exterior ballistics and to investigate whether such theory is applicable to rocket projectiles. For this purpose we consider the motion of a rigid body through the air acted upon by gravity and by air resistance or drag. Assuming negligible yaw, we may represent the air drag by a force acting in the direction opposite to the velocity of the projectile and of magnitude

$$D = -mc\, f(v)$$

where m is the mass of projectile;

c is a constant of proportionality depending on the size, shape and surface of the projectile; it is also called the deceleration coefficient, for the deceleration due to air drag is c f(v);

and f(v) is a function depending upon the velocity, v.

Choosing a coordinate system as in Fig. 2, we have

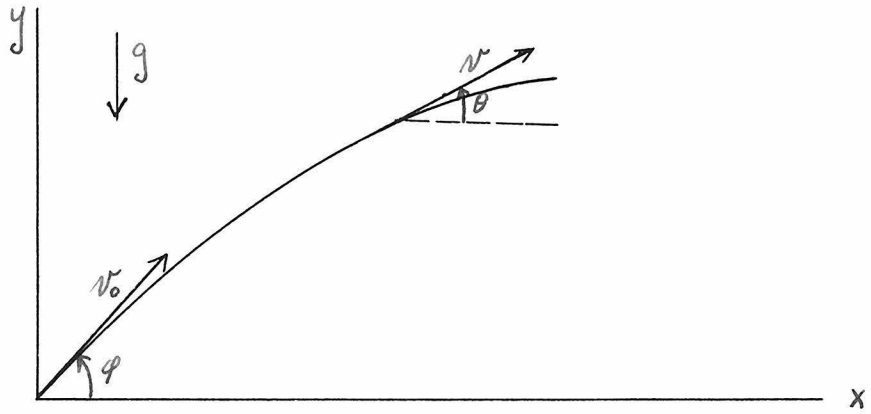

Fig. 2

---

* The following material follows mainly from Cranz, Lehrbuch der Ballistik, Vol. I, wherein a complete description plus computing tables may be found.

for the equations of motion

$$\frac{dv_x}{dt} = -c\, f(v) \cos\theta \qquad (4)$$

$$\frac{dv_y}{dt} = -c\, f(v) \sin\theta - g \qquad (5)$$

where $v_x = v \cos\theta$; $v_y = v \sin\theta$.

The accelerations tangential and normal to the path are given by

$$\frac{dv}{dt} = -c\, f(v) - g \sin\theta \qquad (6)$$

$$\text{and } v\frac{d\theta}{dt} = v^2 \frac{d\theta}{ds} = -g \cos\theta \qquad (7)$$

where $v = \frac{ds}{dt}$, s being the distance along the path.

Eliminating dt from (4) and (7), we have

$$g\, d(v \cos\theta) = cv\, f(v)\, d\theta \ , \qquad (8)$$

which is often referred to as the principal ballistic equation. From (7), we also arrive at the following differential expressions:

Time,	$g\, dt = -v \sec\theta\, d\theta$	(9)
Horizontal Distance,	$g\, dx = -v^2\, d\theta$	(10)
Height,	$g\, dy = -v^2 \tan\theta\, d\theta$	(11)
Path length,	$g\, ds = -v^2 \sec\theta\, d\theta$	(12)

The integration of equations (4) to (12) constitutes the essential problem of so-called exterior ballistics. For c = 0 the above set of equations reduces to the simple equations for the vacuum trajectory, which can be readily integrated. For the more general case many methods of solution* have been proposed, all of which are more or less approximations; for the resistance function f(v) is not in general a simple function of the velocity. Where one is not interested in very great accuracy the quadratic resistance

---

* These are discussed in Cranz and other treatises on exterior ballistics

law (cf. eq. (1)) may be used. However, it is known that this law definitely breaks down at higher velocities (also at very low velocities) for as the velocity of the projectile approaches the velocity of sound the drag increases much faster than v^2. For those special cases, though, in which the velocity of the projectile is less than about 800 ft/sec the quadratic resistance law holds quite well.

B. The Didion-Bernoulli Approximation for the Trajectory:

The object being to apply standard exterior ballistics methods to UP's in free flight (i.e. after the burning period) we shall assume a quadratic resistance law, since the velocities of most rockets developed thus far at CIT are definitely less than 800 ft/sec. Also, to arrive at a solution which can be used with ease we make use of the so-called Didion-Bernoulli approximation.[6] The advantage of this method is that it is straightforward and the results can be applied easily;[7] also, it gives sufficient accuracy for most rockets at present.

From equations (8) and (10) we have

$$dx = - \frac{v \cos\theta \; d(v \cos\theta)}{c \, f(v) \cos\theta} \quad . \qquad (13)$$

The mathematical approximation is to replace $f(v)$ by $f(\alpha v \cos\theta)$ and one $\cos\theta$ (in the denominator) by $1/\alpha$, where the constant α is an appropriate average of $1/\cos\theta$. Also, letting $u = \alpha v \cos\theta$, equation (13) reduces to

$$dx = - \frac{1}{\alpha c} \frac{u \, du}{f(u)} \quad , \qquad (14)$$

which can now be integrated for suitable values of $f(u)$. In the special case of the quadratic resistance law, $f(v) = v^2$,

$$dx = - \frac{du}{\alpha c u} \quad . \qquad (15)$$

As an illustration of the simplicity of the method, let us calculate the time of flight corresponding to any horizontal distance x. Integrating (15),

$$u = K_1 e^{-c\alpha x} = \alpha v \cos\theta \quad .$$

Now making use of the initial conditions that $v = v_o$, $\theta = \phi$ when $x = 0$, we get

$$v \cos\theta = v_o \cos\phi \, e^{-c\alpha x} \quad .$$

Eliminating $d\theta$ from equations (9) and (10) and substituting for $\cos\theta$ from the above,

$$dt = \frac{e^{c\alpha x}}{v_o \cos\phi} \, dx \quad .$$

Integrating and applying the condition that $x = 0$ for $t = 0$, we get

$$t = \frac{1}{v_o \cos\phi} \cdot \frac{e^{c\alpha x} - 1}{c\alpha} \quad .$$

In terms of the dimensionless quantity $\underline{z = 2c\alpha x}$, we have, finally, for the time corresponding to any value of x,

$$t = \frac{x}{v_o \cos\phi} \, D(z) \quad , \qquad (16)$$

$$\text{where } D(z) = \frac{e^{z/2} - 1}{z/2} \quad . \qquad (16a)$$

Similarly, one can derive the following expressions for the elements of the trajectory:

<u>Height along path</u>, $$y = x \tan\phi - \frac{g x^2}{2 v_o^2 \cos^2\phi} \, B(z) \quad , \qquad (17)$$

$$\text{where } B(z) = \frac{e^z - z - 1}{z^2/2} \quad ; \qquad (17a)$$

<u>Tangent to orbit</u>, $$\tan\theta = \tan\phi - \frac{gx}{v_o^2 \cos^2\phi} \, J(z) \quad , \qquad (18)$$

$$\text{where } J(z) = \frac{e^z - 1}{z} \quad ; \qquad (18a)$$

<u>Horizontal component of velocity</u>,

$$v \cos\theta = v_o \cos\phi \cdot V(z) \qquad (19)$$

$$\text{where } V(z) = e^{-z/2} \quad . \qquad (19a)$$

For $c = 0$, it is easy to see that the correction factors $D(z) = B(z) = J(z) = V(z) = 1$; that is, (16), (17), (18), (19) simply reduce them to the elements of the vacuum trajectory. The above D-B method gives a very good approximation to the trajectory for low angles of fire (α very close to unity); but it can also be applied at larger angles if not very great accuracy is desired.

C. Application of Didion-Bernoulli Method to Rocket Trajectories (CIT/JPC 1):

In April 1942 a study was made of the free-flight (i.e., post-burning) trajectories of a group of CWG rockets. Since the velocities were of the order of 500 ft/sec and the quadrant angle of fire only 6°, the D-B approximation is applicable, and this investigation should afford a good test of the applicability of standard exterior ballistics methods to rockets.

Data

The UP's whose trajectories were studied in this investigation were part of a group of 50 CWG (double-web powder) projectiles (Cf. CIT,NMC 1.22-23 (7)) which, as far as possible, were identical in all respects. The firings took place at MAAR on March 28, 1942; and, to secure sufficient photographic data for determining the actual behavior of the UP's in flight, three cameras were placed at different points along the trajectory. These included:

(a) The "CIT" camera, for determining acceleration, velocity, burning distance, and burning time. In the field of view were also two posts (hereafter referred to as M_1 and M_2) situated 25 ft and 50 ft along the range and slightly to one side, which had accurately marked reference points and stripes for determining the heights and angles of yaw of the UP's at these points.

(b) A camera 400 ft along the range for determining the angle of yaw and height at this point (again from a post on range, as in (a)).

(c) A camera 1000 ft along the range for measuring the velocity at this point.

Measurements were made in the usual manner, and, whenever necessary, corrections were made to allow for the fact that the UP and points of reference for measurement (e.g. M_1 and M_2) were not in the same plane but yet were seen in the same plane of projection by the cameras. Only corrected values are given in the accompanying table.

Method

The D-B theory gives the following equation, (17), for the path of the projectile:

$$y = x \tan \phi - \frac{gx^2}{2v_o^2 \cos^2 \phi} B(z) \quad ; \qquad (17)$$

from which $x = \frac{v_o^2 \sin 2\phi}{2g\ B(z)} + \sqrt{\left(\frac{v_o^2 \sin 2\phi}{2g\ B(z)}\right)^2 - \frac{2y\ v_o^2 \cos^2 \phi}{g\ B(z)}}$. (20)

Fig. 3 shows schematically the path of the UP. In general, the UP burned for a short distance (on the average 5.8 ft) beyond the first marker M_1. On the assumption that ϕ does not change measurably over this distance, we use equation (17) for determining ϕ. (That this assumption was valid is borne out by the fact that there is no correlation between ϕ and burning distance; nor are there any systematic differences between observed and computed (from ϕ) ranges as a function of burning distance.)

Thus $$\tan \phi = \frac{y'}{x'} + \frac{g x'}{2v_o^2 \cos^2 \phi} B(z) \qquad (20a)$$

where y' is the difference in the heights of the UP at the two markers and x' is the horizontal distance between the markers. In the last term $B(z) \simeq 1.0015$; and since $\phi < 6^\circ$, $\cos^2 \phi \simeq 0.99$. Therefore,

$$\tan \phi = \frac{y'}{x'} + \frac{gx'}{2v_o^2 (0.99)} \quad , \qquad (20b)$$

from which the values in Table 1 were computed. From the measured values of velocities at the end of burning, v_o, and velocities at 1000 ft along range, v_{1000}, L. Davis has computed the deceleration coefficients, c, (cf. eq. (L), CIT/MTC 3), which are given in column 6. In subsequent computations the mean value of c was used throughout.

The "vertical yaws" are in all cases the angles between the axis of the UP projected on to the vertical plane and the tangent to the trajectory, where θ, the angle of the trajectory, is given by

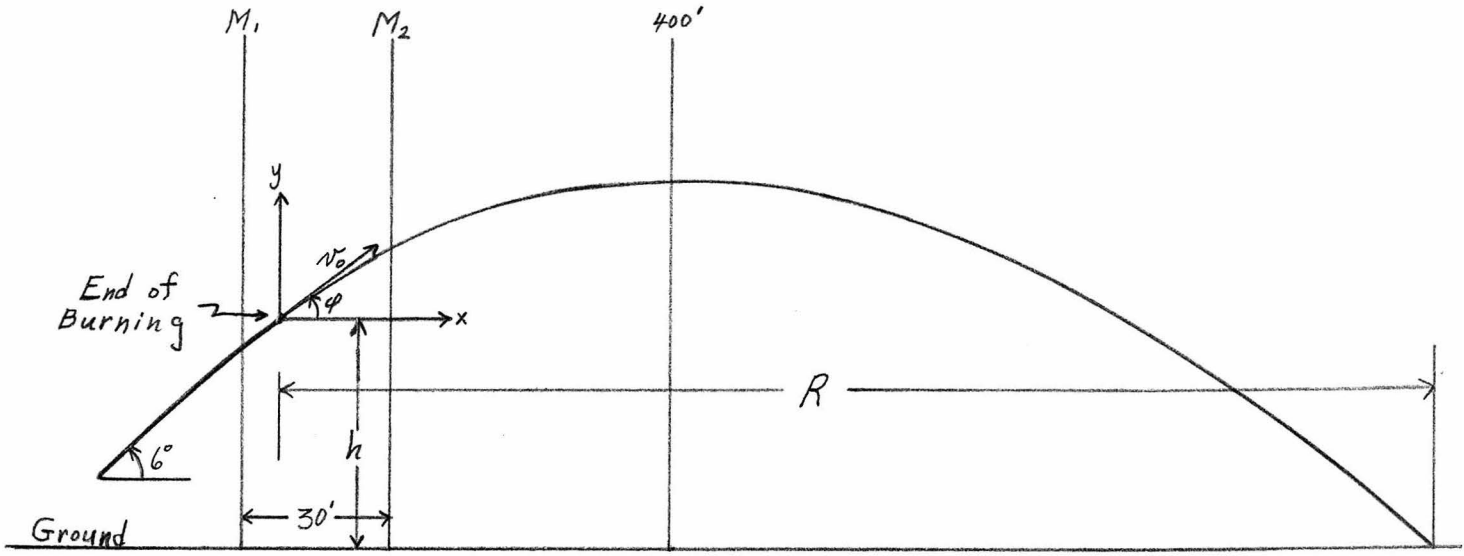

Fig. 3 (Not to scale)

Fig. 4, Departure Angle vs. Yaw at M_2

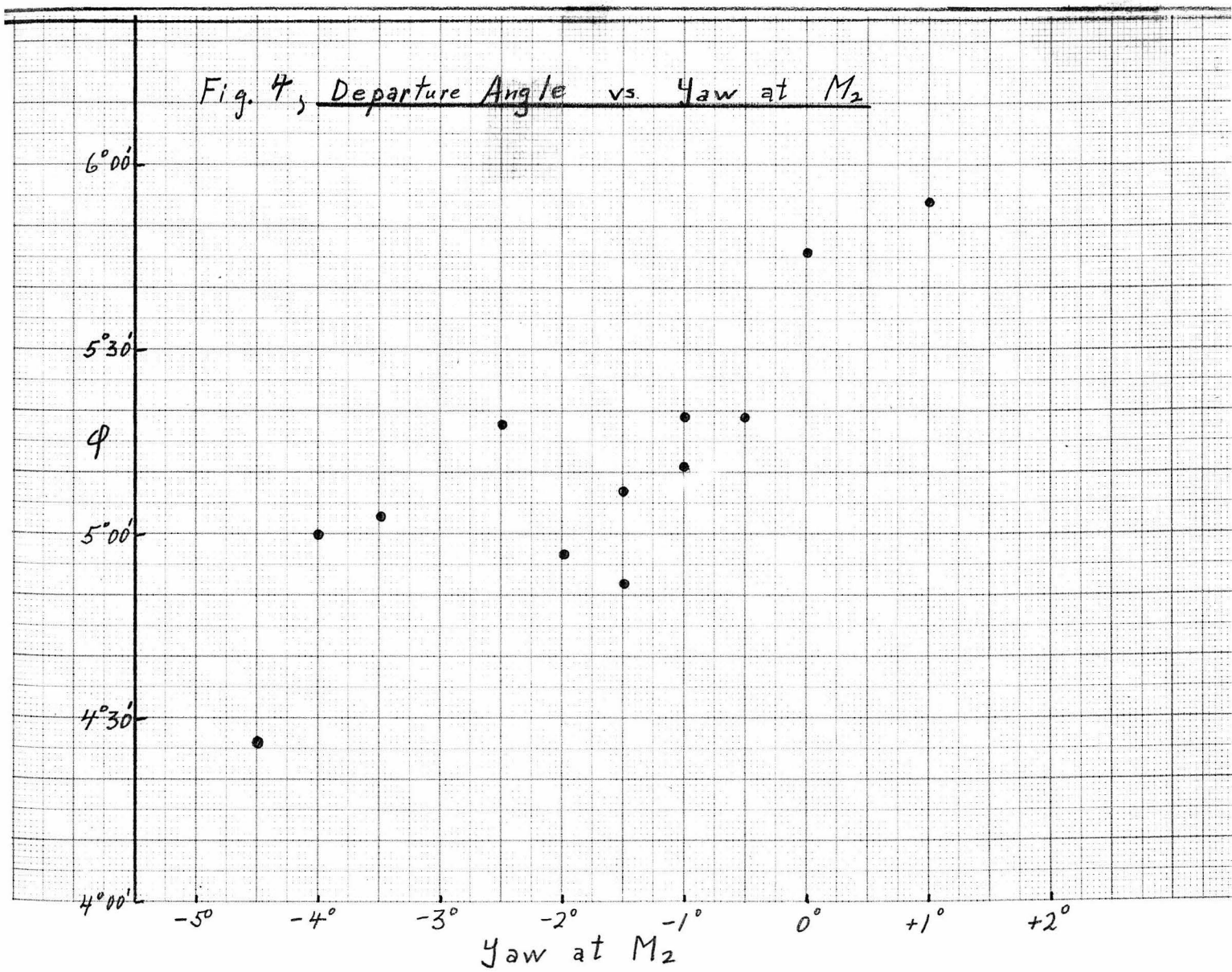

$$\cos \theta = \cos \phi \, (1 - 2gy/v_o^2)^{\frac{1}{2}} \qquad (20c)$$

Equation (20c) holds strictly only for the vacuum trajectory, but in the cases considered here it is practically the same as for the actual path. The heights at 400 ft along range were computed from (17) both for the D-B path and for the vacuum path (with c = 0). Similarly, the "ranges", R, were computed from (20). In all cases R is the total horizontal distance of free-flight.

Results - It is at once apparent (cf. column 1 of table 1) that the departure angles for free flight, ϕ, are in all cases less than the angle (6°) at which the projector was set. The average ϕ is 5° 11' with a random scatter in ϕ about this value. L. Davis has computed (from formulae in CIT/MTC 2) that the maximum change in trajectory angle during burning to be expected for this set of UP's (acceleration $\approx$ 160g; $v_o \approx$ 480 ft sec; burning distance $\approx$ 24 ft; burning time $\approx$ 0.10 sec) is approximately -0.30°, of which about -0.22° is due to the curvature in the trajectory produced by gravity, and the remaining -0.08° is due to the tipping-off produced by the dragging of the tail of the UP on the projector, if this effect is present. The fact that the observed average change is -0.82° indicates that other causes are mainly responsible for this large deviation. The observed angles of vertical yaw at M_1 are too small to be reliable; however, if we compare the angles of yaw at M_2 (which is on the average 23 ft beyond the start of free flight) with the values of ϕ (cf. Fig. 4) we note a decided correlation: The greater the angle of yaw the greater the change in departure angle. This is not unexpected, for any mislaunching or misalignment would produce both vertical deviation (change in ϕ) and vertical yaw in the same direction. From the data, there is no evidence that ϕ is a function of either the burning distance or the burning time.

The most striking result in the table is the unique correspondence between the observed ranges and those computed from the DB theory, and between the observed and computed heights at 400 ft. The mean observed range (1289) is practically the same as the mean D-B range (1286 ft), while the differences between

the observed and DB ranges plainly indicate a random distribution, with 6 positive values and 6 negative. The mean deviation is ± 28 ft, corresponding to a percentage deviation of ± 2%.

Summary - 1. A large unexplained change in the trajectory angle has been found to be introduced during the burning. For the projector set at 6^{o} the average change was found to be -0.8^{o}.

2. The Didion-Bernoulli approximation for the free-flight trajectory is found to hold very well for the CWG projectile having only slight yaw ($< 4^{o}$). Consequently, the post-burning trajectory is identical with that of a shell under the same initial conditions and with the same deceleration coefficient. It follows from (2) that,

3. For the CWG's (with only slight yaw in flight) all effects governing the motion, range, etc. are introduced during burning; and also that the trajectory after burning is sensibly straight, i.e. lies in a vertical plane.

D. Conclusions:

It is reasonable to assume from the above analysis of CWG trajectories that the following deductions may be drawn concerning rockets in general.

1. For rockets having negligible yaw it is quite proper to apply standard methods of exterior ballistics for the post-burning trajectory.

2. All effects governing the motion, range, deflection, etc. of rockets are introduced during the burning period.*

---

* Wind and other extraneous effects are neglected.

Table I

Round	ϕ *	h (ft)	v_o (f/s)	v_{1000} (f/s)	c	"Vertical Yaw" δ_{M_1} (deg)	"Vertical Yaw" δ_{M_2} (deg)	"Vertical Yaw" δ_{400} (deg)	Heights at 400 ft Y_{400} (obs) (ft)	Heights at 400 ft Y_{400} (vac) (ft)	Heights at 400 ft Y_{400} (DB) (ft)	"Ranges" R (obs) (ft)	"Ranges" R (vac) (ft)	"Ranges" R (DB) (ft)	ΔR** (obs-DB) (ft)
5	4° 57'	7.79	490	460	6.6×10^{-5}	$-\frac{1}{2}$	-2	$-\frac{1}{2}$	22.0	22.6	21.9	1313	1371	1289	+24
6	4° 52'	8.01	510	478	6.6	0	$-1\frac{1}{2}$	-2	22.2	22.6	22.0	1388	1454	1360	+28
8	5° 19'	7.53	480	447	8.8	$-\frac{1}{2}$	$-\frac{1}{2}$	$-2\frac{1}{2}$	24.5	24.6	24.0	1321	1394	1310	+11
9	5° 11'	7.71	470	442	6.1	-1	-1	$-2\frac{1}{2}$	22.6	23.1	22.5	1232	1314	1239	-7
10	5° 3'	8.16	485	454	6.7	$-1\frac{1}{2}$	$-3\frac{1}{2}$	+1	20.9	23.4	22.3	1254	1368	1290	-36
12	5° 46'	7.93	505			0	0	$-1\frac{1}{2}$	27.0	28.2	27.6	1493	1661	1546	-53
13	5° 7'	7.71	465	434	7.3	$-\frac{1}{2}$	$-1\frac{1}{2}$	$+\frac{1}{2}$	22.0	22.7	22.0	1220	1277	1202	+18
14	5° 18'	7.01	430			$+\frac{1}{2}$	$-2\frac{1}{2}$	$-\frac{1}{2}$	23.0	22.3	21.6	1104	1129	1071	+33
15	5° 54'	7.59	470			$+\frac{1}{2}$	+1	$-1\frac{1}{2}$	29.8	28.0	27.3	1446	1474	1376	+70
16	5° 19'	8.35	505	466	8.3	0	-1	$+1\frac{1}{2}$	23.8	25.2	24.6	1416	1552	1448	-32
17	5° 0'	7.44	455	421	8.1	-2	-4	0	20.6	21.6	21.0	1118	1199	1139	-21
18	4° 26'	7.60	485	449	8.4	-1	$-4\frac{1}{2}$	+2	18.5	19.2	18.7	1160	1228	1162	-2
Mean	5° 11'	7.74	479		7.4×10^{-5}	$-\frac{1}{2}$	$-1\frac{1}{2}$	$-\frac{1}{2}$	23.1	23.6	23.0	1289	1368	1286	+33

* In all cases, projector was set at 6°
Yaw > 0 for UP pointing up

Mean deviation $\hat{=} \frac{\text{in Range } \sum|\Delta|}{12} = \pm$ 28 ft

** 6 obs. ranges > DB ranges
6 obs. ranges < DB ranges

% deviation = ± 2%

III. Yaw and Deflection Developed During Burning of Rockets (CIT/JPC 3; NDRC, A-164)

A. Causes of inaccuracy of Rockets:

As was shown above, practically all effects governing the range and deflection of rockets are introduced during the burning period. The factors influencing the motion of a UP during this period are many, and it is quite impossible to take them into account all at once. Consequently it will be necessary to limit the problem here to the effect of malalignment alone, the most important of the following factors.

1. Malalignment of the jet. - This is the principle cause of the inaccuracy of rockets; for the failure of the axis of the jet to pass through the center of mass of the projectile causes the UP to rotate during burning about a transverse axis through the center of mass with the result that the direction of thrust of the motor is altered from its initial direction as determined by the projector.

2. Mal-launching. - Improper launching may result in the rocket acquiring an angular velocity as it leaves the rails. The affect of this has been discussed in a paper by L. Davis.[8)]

3. Effects of Gravity. -

a. If the rocket is launched from a projector without an overhead guide, it is free to tip off the end of the projector once the center of gravity of the UP has passed that point. This problem has also been treated by L. Davis.[9)]

b. If the UP were launched without a projector the trajectory during burning would be a straight line. However, the velocity would not be Gt but would be diminished by the amount $gt \sin \theta_0$, approximately. Since, generally, $g \ll G$, this change in velocity is quite negligible. In the usual

case of launching from a projector the effect upon the velocity is about the same. However, the trajectory in this case is no longer straight but has a curvature in the vertical plane.

4. Asymmetry of Projectile Shape. - If the fins, for example, are asymmetrical, they exert a rudder effect upon the UP, thus introducing a yaw and altering the direction of thrust of the rocket motor.

5. Wind. - (This will be discussed in Ch. IV.)

B. Equations of Motion:

We shall assume that the rocket is perfectly symmetrical in shape and is launched properly in a uniform atmosphere free from wind. It will be convenient, too, to neglect the curvature of the trajectory due to gravity during the period of burning. Any errors introduced thereby should be roughly systematic; though one can avoid such difficulties completely by applying the results to yaw and deflection in a plane perpendicular to the vertical, wherein gravity plays a negligible role.

The remaining forces then are the thrust of the malaligned jet and the aerodynamic forces and torques. The air drag will decrease the velocity of the rocket roughly by the amount $\Delta v = \int cv^2\,dt = \frac{1}{3}\, c\, v_b^{\,2}\, t_b$. Since $c \simeq 5 \times 10^{-5}$ ft^{-1} for practically all UP's at CIT, and $v_b\, t_b \simeq 2 \times 10^2$ ft, the loss in velocity due to drag is of the order of less than one percent. The cross-wind force has the effect of displacing the UP normal to the trajectory. However, the (malaligned) jet also has a component of force perpendicular to the trajectory. Assuming, as a first approximation for small yaw, that the cross-wind force is given by $L = D\delta$, the ratio of the cross-wind force to the component of the thrust perpendicular to the trajectory is

$$\frac{L}{mG\delta} = \frac{m\, c\, v^2 \delta}{m\, \delta\, v_b/t_b} \leq c\, v_b\, t_b \simeq .01 \quad .$$

Consequently, the cross-wind force, as well as the drag, may be neglected during the period of burning.*

For the aerodynamic restoring torque of our finned rocket, we have, from eq. (3),

$$M = K_M \rho d^3 v^2 \sin\delta = K v^2 \delta \quad ,$$

where K has been substituted for $K_M \rho d^3$ and δ for $\sin\delta$.

For the resistance to angular motion we assume a damping couple, $-\mu \dot{\phi}_c$, proportional to the angular velocity. Though the damping coefficient, μ, is some function of velocity, we shall not consider this dependence, since our only concern is with the order of magnitude of the damping. All we assume is that μ remains constant at some fixed velocity.

The effect of the jet is conveniently resolved into two parts: a resultant force F which accelerates the center of mass, and a torque which produces a rotation about the center of mass. We express this torque as F L(t), where L, the malalignment is the distance that the center of mass must be from F if the force F and the lever arm L are to produce the required torque.

Under the above restrictions, the motion of the UP is in the "plane of yaw" determined by the projector and the direction of the axis of the jet.

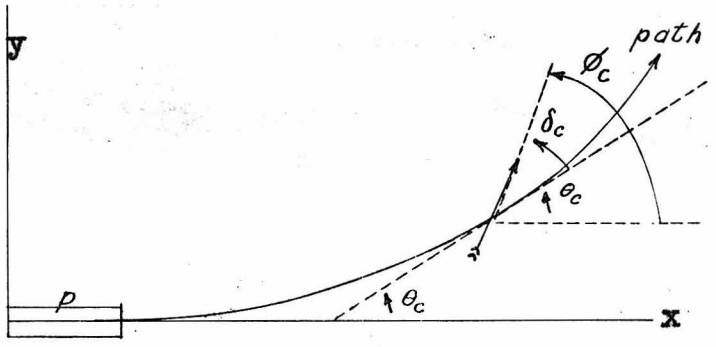

Fig. 5

---

* We have neglected the fact that the malalignment itself of the jet introduces an additional component to the force normal to the trajectory. This, however, is quite unpredictable from round to round. The evidence is that this effect is unimportant.

The angles in this plane (cf. Fig. 5) are designated with the subscript "c" to distinguish the symbols from their usual meanings.

The complete equation for the rotation of the projectile is then

$$I \ddot{\phi}_c = F\,L(t) - K v^2 \delta_c - \mu \dot{\phi}_c \quad . \qquad (21)$$

The curvature of the trajectory is caused by the component of F perpendicular to the trajectory. Equating the centrifugal force to this gives

$$mv \dot{\theta}_c = F \delta_c \quad . \qquad (22)$$

Also $$\phi_c = \theta_c + \delta_c \quad ; \qquad (23)$$

where ϕ_c = angle between axis of UP and initial direction on projector in plane of yaw

θ_c = angle between tangent to trajectory and initial direction (θ_c = deflection in plane of yaw)

$\delta_c = \phi_c - \theta_c$ = yaw of projectile

m = mass of projectile

k = radius of gyration about transverse axis through the CG

$I = mk^2$ = moment of inertia about transverse axis through CG

L(t) = malalignment of jet. If the malalignment is considered independent of time, this becomes L_o.

G = linear acceleration of rocket during burning

F = mG = force propelling rocket

t = time from start of burning

v = Gt = velocity of rocket

K = moment coefficient of fins; restoring torque = $K v^2 \delta_c$

μ = damping coefficient; damping moment = $\mu \dot{\phi}_c$

During the post-burning period, F = o and $v = v_b$ = const.; thus (21) and (22) reduce to

$$I \ddot{\delta}_c = -K v_b^2 \delta_c - \mu \dot{\delta}_c \qquad (24)$$

an equation for damped oscillation with period

$$T = \frac{2\pi}{\left(\frac{Kv_b^2}{I} - \frac{\mu^2}{4I^2}\right)^{\frac{1}{2}}} \qquad (25)$$

The damping coefficient μ is given by

$$\mu = \frac{2I}{T} \ln \frac{A'}{A''} \qquad (26)$$

where A' and A" are two successive amplitude crests on the yaw curve ($\ln A'/A''$ = logarithmic decrement). Thus μ can be determined from the period and shape of the observed yaw curves; and K, from (4), is given by

$$K = \frac{4\pi^2 I}{v_b^2 T^2} + \frac{\mu^2}{4v_b^2 I} \qquad (27)$$

In general, the yaws are too small to be able to determine μ. However, for the Chemical Warfare Grenade (CWG) with a built-in malalignment (to produce large yaws; see CIT/MTC 7) μ was found to be 1.1* at a velocity of 325 ft/sec. With this value of μ, the second term on the right-hand side of (27) is about 10^{-3} times the first term. For the slower-moving projectiles (such as the ASPC Mk. projectile or Beach Barrage Rocket Mk. 1), even if μ is as much as ten times that for the CWG, the second term in (27) is about 10^{-2} times the first and so is again negligible. Thus we can write

$$K = \frac{4\pi^2 I}{v_b^2 T^2} \qquad (28)$$

from which formula K was actually determined. (For variation of K with fin size, see the experimental results for the CWG at the end of this report.)

It is more convenient to express the effect of the fins in terms of the distance σ traversed by the rocket in free flight while the yaw oscillates through one full cycle. Thus, from (28),

$$\sigma = v_b T = 2\pi \sqrt{\frac{I}{K}} \quad . \qquad (29)$$

---

* Except where specified, absolute fps units are used throughout.

Since, as indicated above, the damping moment $-\mu\dot{\phi}_c$ is considerably smaller than the aerodynamic torque $-Kv^2\delta_c$ (and also to facilitate a solution of the equations) we neglect this term in equation (21). Rewriting (21), (22) and (23), we then have

$$\ddot{\phi}_c = \frac{GL(t)}{k^2} - \frac{4\pi^2 G^2 t^2 \delta_c}{\sigma^2} \qquad (30)$$

$$t\dot{\theta}_c = \delta_c \qquad (31)$$

$$\phi_c = \theta_c + \delta_c \qquad (32)$$

In writing $v = Gt$, we assumed that the acceleration of the projectile, G, is constant during burning (that is, $G = v_b/t_b$), which, though a rash assumption in some cases, should nevertheless yield approximately the same results.* The boundary conditions on this set of equations are that at $t = t_p$ (the time that the rocket leaves the projector), $\delta_c = \dot{\delta}_c = \phi_c = \dot{\phi}_c = 0$.

C. Solution of Equations and General Conclusions:

As is pointed out in appendix 1, results from the yaw machine indicate that the malalignment of the jet is far from constant during burning, but rather may vary considerably. (In the appendix the torque produced by the jet is expressed in terms of the side force acting at the nozzle instead of the malalignment of the resultant jet force, but the two descriptions of the torque are, of course, equivalent.)

Since a solution with a malalignment which is an arbitrary function of time can only be given in the form of a definite integral, we will con-

---

* In CIT/ITC 2, L. Davis has shown that the dispersions in vacuo are essentially the same for various types of burning.

sider three simple special cases. By solving equations (30), (31) and (32) for these forms of L(t) we should get a satisfactory understanding of the behavior of the projectile in general.

Case I: $L(t) = L_o$.*

Here we assume constant malalignment during burning (that is, constant upsetting torque). The solutions are conveniently expressed in terms of the dimensionless quantity $z = \sqrt{2\pi G/\sigma}\, t$,

or $z = \sqrt{\frac{2\pi v_b}{\sigma t_b}}\, t = \sqrt{4\pi s/\sigma}$.

We have

$$\delta_c = \frac{\sigma L_o}{2\pi k^2} \cdot \frac{1}{z} \left(\delta_o + A_1 \delta_1 + A_2 \delta_2\right) \tag{33a}$$

$$\phi_c = \frac{\sigma L_o}{2\pi k^2} \left(\phi_o + A_1 \phi_1 + A_2 \phi_2 + A_3\right) \tag{33b}$$

$$\theta_c = \phi_c - \delta_c \tag{33c}$$

where

$$\phi_o(z) = \frac{1}{2}\left[\phi_1{}^2(z) + \phi_2{}^2(z)\right] \text{**} \tag{34a}$$

$$\phi_1(z) = -\sqrt{\pi}\, S(z/\sqrt{\pi}) \tag{34b}$$

$$\phi_2(z) = \sqrt{\pi}\, C(z/\sqrt{\pi}) \tag{34c}$$

$$\delta_o(z) = \phi_1(z)\cdot\delta_1(z) + \phi_2(z)\cdot\delta_2(z) \tag{34d}$$

$$\delta_1(z) = \cos z^2/2 \tag{34e}$$

$$\delta_2(z) = \sin z^2/2 \tag{34f}$$

$$A_1 = -\phi_1(z_p) \tag{34g}$$

---

* The author is greatly indebted to Dr. Leverett Davis for this solution and for indicating the method of solution for Cases II and III. (See appendix 2.)

** Developed by Dr. Morgan Ward.

$$A_2 = -\phi_2(z_p) \qquad (34h)$$

$$A_3 = \phi_o(z_p) \qquad (34i)$$

$z_p = \sqrt{2\pi G/\sigma} \cdot t_p = \sqrt{4\pi p/\sigma}$ is the value of z when $t = t_p$, and p is the effective projector length; that is, the distance the rocket moves before the constraint of the rails is removed.

The functions $C(z/\sqrt{\pi})$ and $S(z/\sqrt{\pi})$ are the Fresnel Integrals.

Case II: $L(t) = \frac{L'_o}{t_b} t$.

Here we assume that the malalignment (or upsetting torque) increases linearly with time. The solutions are

$$\delta_c = \frac{\sigma L'_o}{2\pi k^2 z_b} \cdot \frac{1}{z}(1 + B_1\delta_1 + B_2\delta_2) \qquad (35a)$$

$$\phi_c = \frac{\sigma L'_o}{2\pi k^2 z_b}(B_1\phi_1 + B_2\phi_2 + B_3) \qquad (35b)$$

$$\theta_c = \phi_c - \delta_c \quad . \qquad (35c)$$

where δ_1, δ_2, ϕ_1 and ϕ_2 are the same as in case I,

$$B_1 = -\delta_1(z_p) \qquad (35d)$$

$$B_2 = -\delta_2(z_p) \qquad (35e)$$

$$B_3 = \delta_o(z_p) \qquad (35f)$$

and z_p and z_b are the values of z when $t = t_p$ and $t = t_b$, respectively.

Case III: $L(t) = L'_o\left(1 - \frac{t}{t_b}\right)$.

Here we assume that the malalignment (or upsetting torque) decreases linearly from a maximum value L'_o at $t = 0$ to zero at $t = t_b$. This approximation to L(t) fits most closely the preliminary data yielded by the yaw machine.

The solutions are

$$\delta_c = \frac{\sigma L'_o}{2\pi k^2 z_b} \cdot \frac{1}{z} (z_b \delta_o + a_1 \delta_1 + a_2 \delta_2 - 1) \quad (36a)$$

$$\phi_c = \frac{\sigma L'_o}{2\pi k^2 z_b} (z_b \phi_o + a_1 \phi_1 + a_2 \phi_2 + a_3) \quad (36b)$$

$$\theta_c = \phi_c - \delta_c \quad (36c)$$

where ϕ_o, ϕ_1, ϕ_2, δ_o, δ_1, δ_2 are the same as in Case I,

$$a_1 = \delta_1 (z_p) - z_b \phi_1 (z_p) \quad (36d)$$

$$a_2 = \delta_2 (z_p) - z_b \phi_2 (z_p) \quad (36e)$$

$$a_3 = z_b \phi_o (z_p) - \delta_o (z_p) \quad (36f)$$

and z_p and z_b are the values of z when $t = t_p$ and $t = t_b$, respectively.

In the following analysis it will be assumed that the malalignment of the jet is constant during burning (Case I). Though this condition can hardly be expected to prevail, nevertheless the three types of malalignment discussed above yield essentially the same yaws and deflections. The value of θ_c/L_o for $t = t_b$ is a measure of the deflection to be expected, since under our hypotheses θ_c remains constant after burning.

If we take as the "plane of yaw"* the plane passing through the projector, and perpendicular to the vertical plane through the projector, and if θ_o is the quadrant angle of the projector, then the lateral deflection on range, β, is given by

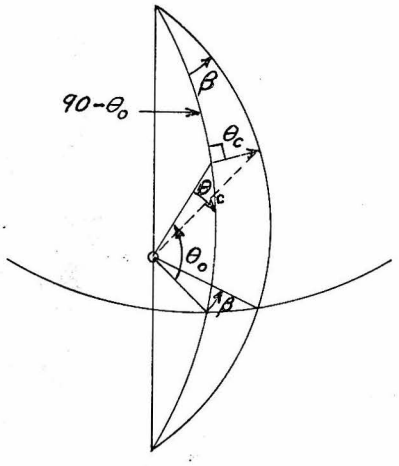

Fig. 6

* This is taken as the plane of yaw mainly because we can easily compare predicted dispersions in this plane with the observed lateral dispersions on range.

$$\tan \beta = \frac{\tan \theta_c}{\cos \theta_o}$$

or, since β and θ_c are small,

$$\beta = \frac{\theta_c}{\cos \theta_o} \quad . \qquad (37)$$

(i) Fig. 7 is a graph of $k^2 \theta_c / \sigma L_o$ as a function of $Z/\sqrt{2\pi}$ $(= \sqrt{G/\sigma}\, t)$. These curves may therefore be used to give the angle between the rails and the trajectory at any point during the burning period. If one is interested in the deviation of the final trajectory after the completion of burning, the expression for this may be obtained by substituting the burning time t_b for $\underline{t}$, since the slope of the curve at this time determines the final direction of the projectile; $Z/\sqrt{2\pi}$ therefore becomes $Z_b/\sqrt{2\pi} = \sqrt{G/\sigma} \cdot t_b$. Since $G = v_b/t_b$, this may further be simplified to $\sqrt{v_b t_b/\sigma}$. Furthermore, since $\sigma / v_b = T$, the period of oscillation in free flight, $Z/\sqrt{2\pi}$ may also be expressed as $t/\sqrt{T t_b}$ and $Z_b/\sqrt{2\pi}$ as $\sqrt{t_b/T}$. The upper scale in Fig. 7 indicates the value of $\sqrt{G/\sigma} \cdot t$ and holds at all times; while the lower scale gives the value of $v_b t_b/\sigma = t_b/T$, and in this form refers only to the end of burning. The upper scale is therefore used when considering the variation of θ_c/L_o with time when the acceleration $\underline{G}$ is fixed. The lower scale will be more convenient for determining the value at the end of burning of θ_c/L_o as a function of burning time when the final velocity of the rocket remains constant.

From these curves it is evident that the accuracy is only slightly dependent on the burning time t_b if this time exceeds $\underline{T}$, the period of oscillation of the projectile in free flight; or, in other words, if the burning distance $\frac{1}{2} v_b t_b$ exceeds $\frac{1}{2}\sigma$.

(ii) In Fig. 8 the results of the same solution (Eqs. (33a), (33b), and (33c)) are plotted so as to show more clearly the conditions under which fin size is of importance. In this figure the abscissa is again the

ratio t_b/T. The ordinate is the ratio of the dispersion for the given value of t_b/T to the dispersion that would have been attained if $\underline{T}$ were infinite -- that is, if only enough fin surface were present to give the rocket neutral stability in free flight. Curves are given for several projector lengths. While $\underline{T}$ depends on $\underline{I}$, the moment of inertia of the projectile, the latter factor is ordinarily fixed by other considerations of design. Consequently, the only practical method for varying $\underline{T}$ is to change the size or position of the fins. The second set of abscissas is given to show the variation with $\underline{K}$, the fin coefficient. In cases in which $p/v_b t_b < 0.10$ -- that is, in which the projector length is less than one-fifth of the burning distance -- the results in Fig. 8 may be roughly summarized as follows.

Fins of such size as to make the period of vibration equal to the burning time decrease the dispersion to about 70 percent of the dispersion with no fins or, more rigorously, with fins just large enough to give the rocket neutral stability. For fins of greater size the dispersion is roughly proportional to the period of oscillation in free flight produced by the fins.

(iii) In Fig. 9 the effects of projector length on dispersion are similarly shown. The abscissa is the ratio of effective projector length $\underline{p}$ to $v_b t_b$, where $v_b t_b$ is twice the burning distance. The ordinate is the ratio of dispersion for the given value of $p/v_b t_b$ to the dispersion for zero projector length. Curves are given for various values of t_b/T. For projector lengths between 0.01 and 0.50 times the burning distance, the decrease in dispersion is roughly linear with the logarithm of the effective projector length.

From Table 2 which lists the constants of a number of projectiles that have been developed on this project, it is evident that fins of a size found practical for use yield a value of about 200 to 300 ft for σ and a

value of $200/v_b$ to $300/v_b$ sec for T. Hence, for projectiles such as the mousetrap and the barrage rocket, whose speeds are less than about 500 ft/sec, $t_b << T$; and therefore the burning time is the important factor in determining dispersion whereas fin size has very little effect. On the other hand, for projectiles with higher velocities, $t_b >> T$, and therefore the fin size has a large effect on accuracy while the burning time does not play an appreciable role.

D. Limitations of the Theory:

It should be emphasized that L(t) is the distance from the axis of thrust of the gas jet to the center of mass of the rocket and that this is not necessarily the same as the distance from the geometric axis of the nozzle to the center of mass. Because of dissymmetry in the burning of the powder or irregularities along the path of the jet that may introduce turbulence or shock waves into the flow of the gas, the axis of this flow may deviate from the geometric axis of the nozzle. Indeed, a considerable body of evidence has developed that indicates that such deviations may be as large as or larger than the geometric malalignment of the nozzle. Furthermore, deviations of this type may vary rapidly during the burning period rather than remain constant, as was assumed in the foregoing solution. All of this means that the absolute values of the dispersions calculated on the basis of Fig. 7 and the measured geometric malalignments can be relied on only as to order of magnitude.

While these uncertainties may affect the estimated, absolute values of the dispersion, they should not appreciably change the relative dispersions to be expected when fin size or burning time is varied for a given projectile. If anything, the dispersion should vary somewhat more rapidly with projector length than is indicated by Fig. 9, since such evidence as is

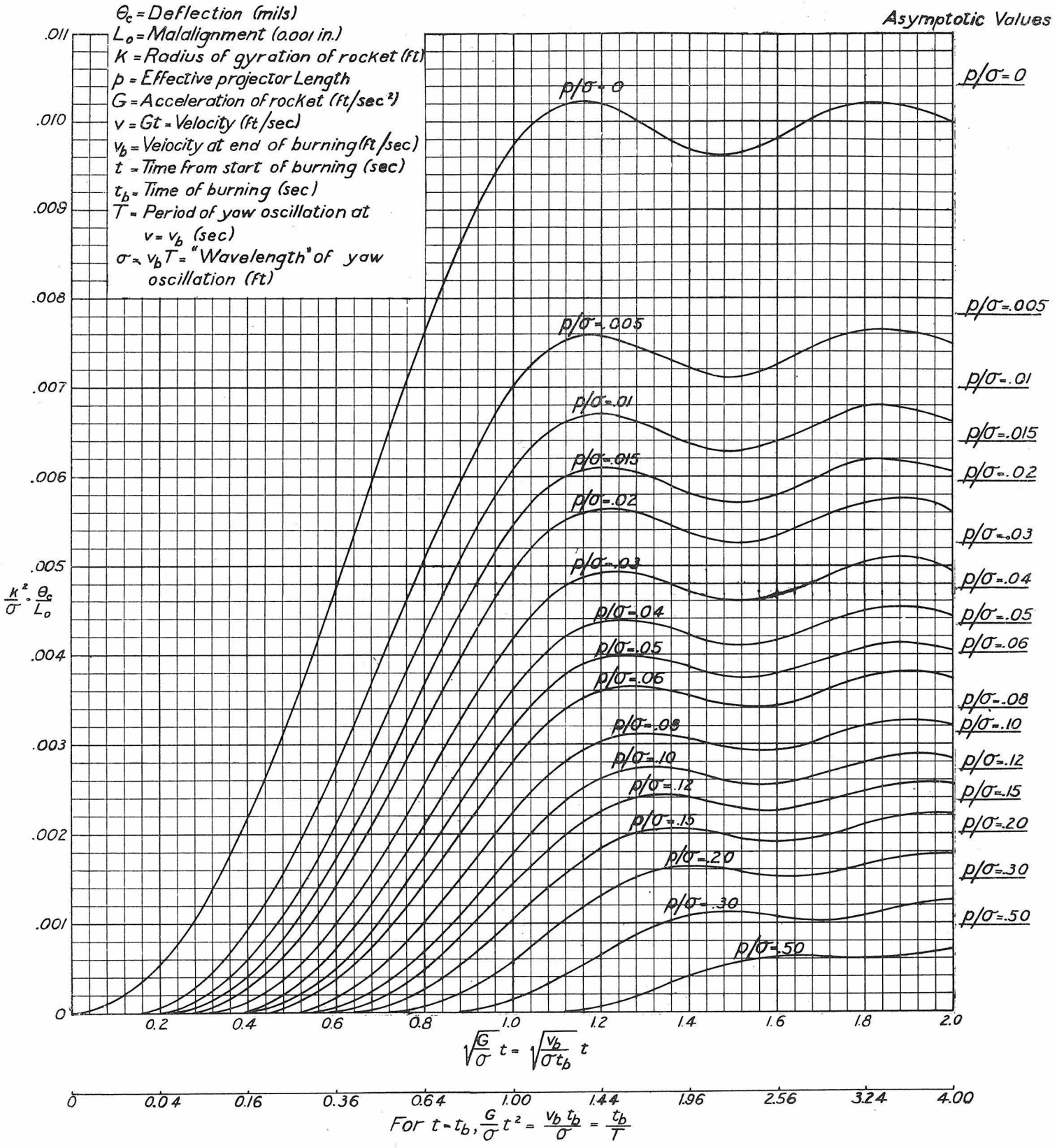

Fig. 7

DEFLECTION OF TRAJECTORY IN PLANE OF YAW

Fig. 8

Effect of Fins on Deflection of Rockets

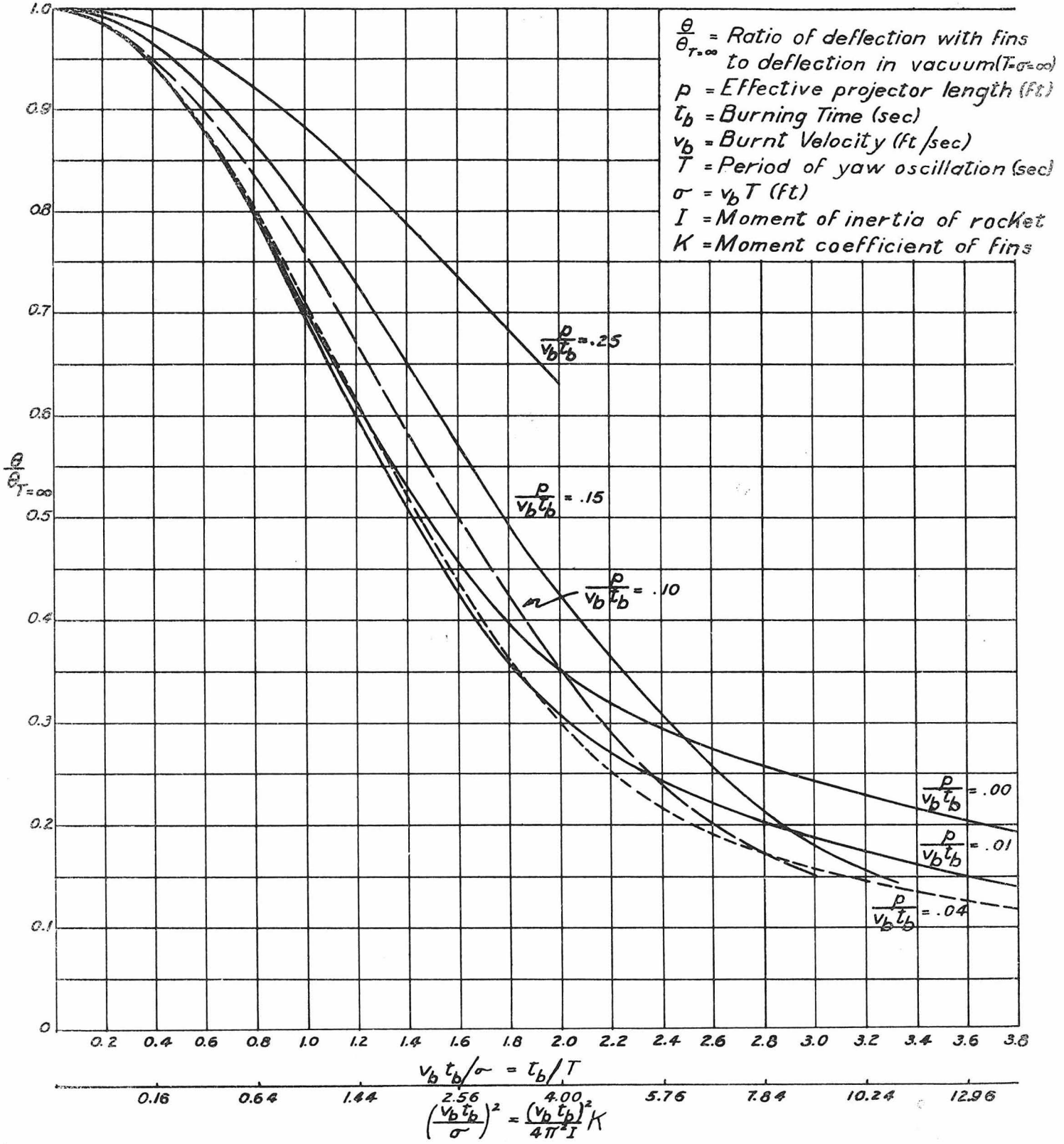

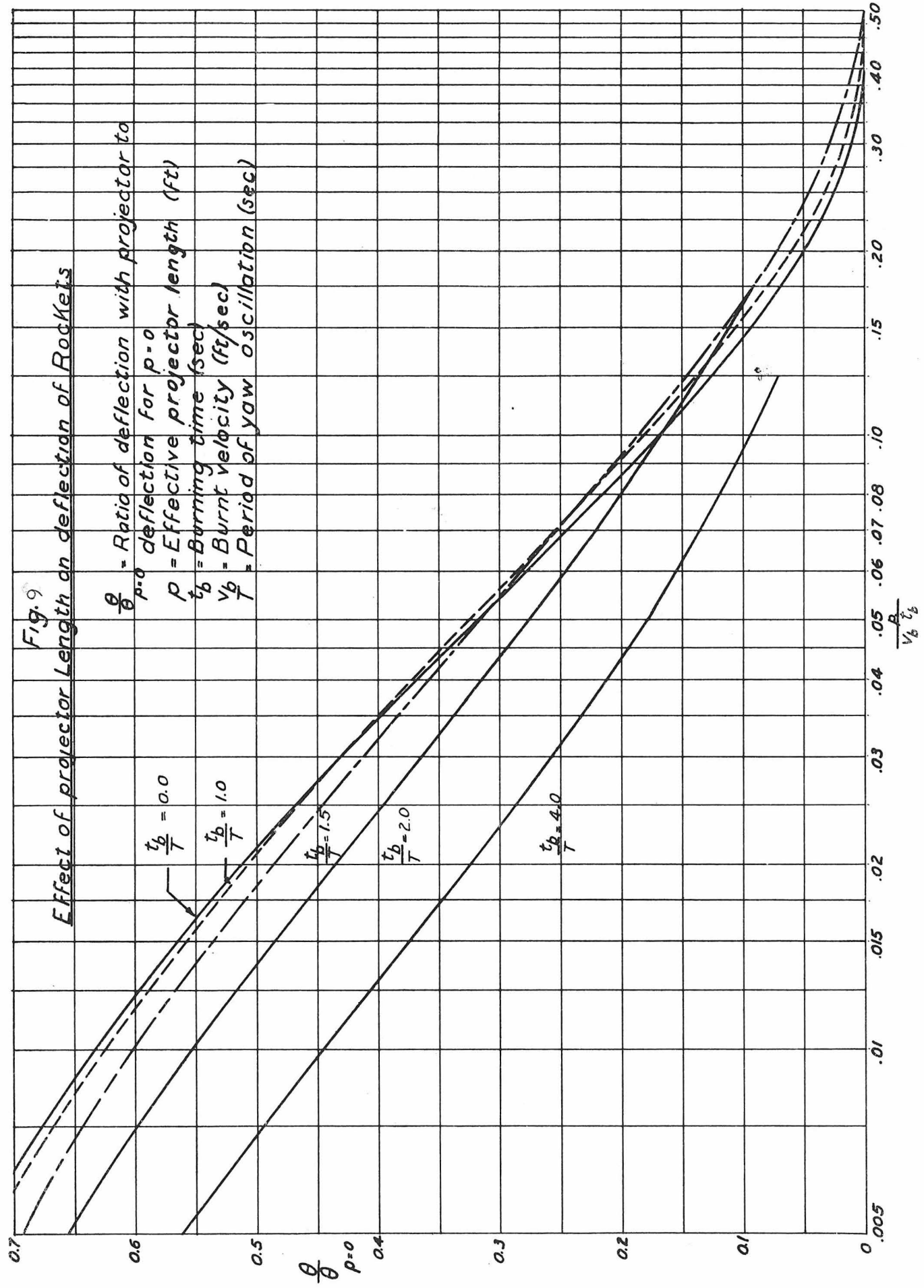
Effect of projector Length on deflection of Rockets
$\frac{\theta}{\theta_{p=0}}$ = Ratio of deflection with projector to deflection for p-0
p = Effective projector length (ft)
t_b = Burning time (sec)
$\frac{v_b}{T}$ = Burnt velocity (ft/sec)
T = Period of yaw oscillation (sec)
$\frac{t_b}{T}$ = 0.0
$\frac{t_b}{T}$ = 1.0
$\frac{t_b}{T}$ = 1.5
$\frac{t_b}{T}$ = 2.0
$\frac{t_b}{T}$ = 4.0
$\frac{\theta}{\theta_{p=0}}$
$\frac{p}{v_b t_b}$
0.7
0.6
0.5
0.4
0.3
0.2
0.1
0
.005
.01
.015
.02
.03
.04
.05
.06
.07
.08
.10
.15
.20
.30
.40
.50

Fig. 9

Table II. Constants of various rockets

		v_b (ft/sec)	t_b (sec)	p (ft)	m (lb)	k^2 (ft^2)	I (lb ft^2)	T (sec)	σ (ft)	K (10^{-3} lb)	$v_b t_b$ (ft)	t_b/T	p/σ	$p/v_b t_b$
Chemical warfare grenade	Small fins*	764	0.22	3.5	2.70	0.346	0.93	0.28	213	0.82	168	0.79	0.016	0.021
	Std. fins	326	.092	3.5	2.74	.346	.95	.49	160	1.51	30	.19	.022	.116
	Std. fins	754	.23	3.5	2.74	.346	.95	.24	177	1.23	173	.98	.020	.020
	Std. fins	774	.23	3.5	2.74	.346	.95	.22	172	1.33	178	1.04	.020	.020
	Med. fins*	739	.22	3.5	2.86	.360	1.03	.16	115	3.15	162	1.42	.030	.022
	Large fins*	662	.22	3.5	3.06	.402	1.23	.14	91	5.92	146	1.58	.039	.024
Chemical warfare bomb		720	0.47	8	47	1.48	69.5	0.40	285	34	338	1.19	0.028	0.024
4.5-in. barrage rocket		360	.32	3.5	27	0.434	11.7	.70	250	7.4	115	0.46	.014	.030
Fast-burning barrage rocket		335	.20	3.3	28.3	.69	19.5	.81	270	10.6	67	.25	.012	.049
Mousetrap		175	.34	4.5	56	.39	21.8	.94	165	31.6	59.5	.36	.027	.076
Subcaliber mousetrap		175	.20	5	8.5	.14	1.19	.86	150	2.0	35	.23	.033	.143

* Experimental rockets not adapted for actual use.

available suggests that the malalignment of the gas jet is greater near the start of burning that it is at later times.

In setting up the equations of motion it was assumed that the restoring force of the fins is proportional to the square of the velocity. This law seems to be applicable until the velocity of the rocket approaches the velocity of sound, but definitely breaks down for higher velocities. For these higher velocities the restoring force is, if anything, larger than that given by the v^2 law. If, therefore, the projectile has reached the flat portion of the curve in Fig. 7 by the time a velocity of 800 ft/sec is reached, we may assume that these curves are correct for any final velocity, since, according to the law of force assumed, the force is already large enough to prevent further appreciable deviation. In other words, if the distance required to attain a velocity of 800 ft/sec exceeds $\frac{1}{2}\sigma$, where σ is the distance covered in one period of free flight, the curves are approximately valid for any velocity. In this case the value of σ for the projectile should be determined for a speed less than 800 ft/sec.

In addition, the restrictions on gravity, cross-wind, drag, etc. put further limits on the theory, though these latter effects are second-order compared to the effect of malalignment. Dr. Bowen has recently pointed out that during burning the gas jet sucks a considerable amount of air past the fins, and therefore the air velocity immediately adjacent to the fins is greater than the velocity of the rocket. Exactly what the effect of this is is not known at present, but it might be significant.

E. Comparison Between Observed and Predicted Results:

Most of the experimental study on the development of yaw during burning has been made with the CWG (Chemical Warfare Grenade), and consequently this projectile is used for the following detailed analysis.

Flight tests of the CWG have been made with four different sizes of fins. The values of K and σ for these sets of fins are given in Table 3. Fig. 10, in which K is plotted as a function of the area of the fins, seemingly indicates that the moment coefficient is about proportional to the fin area. Though this might not be unexpected for the three smaller fins, for which only the widths are different, it is probably a coincidence, because of the particular dimensions of the large fins, that they too seem to fit the linear relation. We also note (for the standard fins) that K does not seem to depend upon the velocity of the projectile in the range of velocities considered.

To illustrate the shapes of yaw and deflection curves, in Fig. 11 δ_c/L_o and θ_c/L_o are plotted as functions of time for the single-web CWG with standard size fins, on the assumption of constant malalignment, $L(t)=L_o$. The curves are continued beyond the usual burning time merely to illustrate the effects of prolonged burning. The plotted circles (taken from CIT/MTC 5) in the figure are values of the yaw observed when an abnormally large malalignment was introduced. The scale of the yaw has been adjusted to give a fit with the theoretical curve near the start of burning. If it were possible to determine the functional form of L(t) in any case, one could get a value for the malalignment constant L_o by fitting the observed yaw curve to the theoretical curve. In any event, by fitting the initial portions of the curves it is possible to determine L_o in this region. This then gives an estimate of the initial malalignment or the initial side force at the nozzle throat. (See Table 3 for values.) In Fig. 11 θ_c/L_o (dashed curve) is also plotted for the multi-web CWG. Since for a given malalignment the overturning moment FL(t) is proportional to the acceleration G, we note as expected that the multi-web veers off at a greater rate than the single-web.

The leveling off at the different values of θ_c/L_o is due to the fact that slightly different effective projector lengths were taken in the two cases.

In Fig. 12 the deflections θ_c/L_o are plotted as a function of K for both low (400 ft/sec) and high (800 ft/sec) velocities, and also for two different burning times at the higher velocity. As expected, the effect of fins on accuracy is much greater at 800 ft/sec than at 400 ft/sec, and in fact the deflection at the lower velocity does not depend much on K at all. It is important to note, too, that where fins do play an appreciable role (800 ft/sec) the dependence of θ_c on K is greater the longer the burning time.

Except for yaw studies in which abnormally large geometrical malalignments were introduced, the only range tests with other than standard fins were made with the large fins. In Table 4 we have some data on the observed and predicted dispersions for identical firings, in which only the fin sizes were different. If we assume that the average malalignments were the same in the two cases, we find that the ratio of dispersions (small fins to large fins) is observed to be 1.8, while the predicted value is 2.4, of the same order of magnitude.

To illustrate the observed effect of burning time on accuracy, some recent field-test determinations of θ_c/L_o for the 4.5 in. BR (Barrage Rocket) are shown in Fig. 13. (From Fig. 6, CIT/IBC 23) Each point represents one test, the number of rounds differing for each. The theoretical curve was calculated by means of the master curves in Fig. 7 using the data for this projectile as given in Table 2. In spite of the fact that the points represent a heterogeneous collection (cf. CIT/IBC 23. There were often changes in design of nozzle, etc. from one test to the next.) The agreement between the observed and predicted values seems rather good.

Table 3

Summary of Fin Coefficients for the CWG

Fins	Size (in.)	m (lb)	I ($lb\text{-}ft^2$)	v_b (ft/sec)	T (sec)	σ (ft)	K [pdl ft/ $(ft/sec)^2$/ rad]
Small	4x5/8	2.70	0.93	764	.278	213	0.82×10^{-3}
Standard	4x15/16	2.74	0.95	326	.49	160	1.51×10^{-3}
"	"	"	"	754	.235	177	1.23×10^{-3}
"	"	"	"	774	.222	172	1.33×10^{-3}
Medium	4x2	2.86	1.03	720	.153	110	3.36×10^{-3}
"	"	"	"	758	.157	119	2.93×10^{-3}
Large	$6x2\frac{1}{2}$	3.06	1.23	662	.139	91	5.92×10^{-3}

Average initial malalignment (from yaw curves) $\simeq$ .055 in.
Average initial side force (from yaw curves) $\simeq$ 41 pdls

Table 4

Comparison of Dispersion for Different Fins

Date	Type of Fins	No. of Rounds	Obs. Dispersion	t_b (sec)	v_b (ft/sec)	Predicted θ_c/L_o
42-04-18	Standard	4 SW	26.4 mils	.21	750	2.4
42-04-18	Large	7 SW	14.4	.21	750	1.0

Observed Ratio of Dispersions = 1.8

Predicted Ratio of Dispersions = 2.4

Perhaps the most beautiful demonstration of the correlation between deflection and malalignment is the result of a recent set of firings of 4.5 in. BR's, in which the motors had excessively large geometrical malalignments. Fig. 14 is a plot of the observed lateral deflections against the corresponding malalignment. The straight line is the theoretically expected slope, on the basis of geometrical malalignment alone, which fits the observed points remarkably well. This correlation between deflection and malalignment is much better than is usually obtained, the reason being that the "gas" malalignments in this case are much smaller than the (abnormally large) geometrical malalignments. In the usual case, however, the gas malalignments are as large as, and quite often larger than, the geometrical malalignments; so that the predicted deflections are considerably altered. The important point, though, is that the effect of the "gas" malalignment is relatively much greater when the geometrical malalignments are small than when they are large. The presence of this "gas" malalignment effectively establishes a lower limit to the accuracy of rocket fire.

F. Conclusions:

Because of the many simplifying assumptions made in setting up the equations of motion, it is not to be expected that the theory will predict deflections to any high degree of accuracy. It is difficult even to estimate probable error, for this depends to a very great extent upon the relative magnitudes of the geometrical malalignment and the "gas" malalignment. In the usual case a 20-25% probable error might perhaps be representative.

The most useful purpose of the theory is for predicting the relative effects of varying burning time, projector length or fin size on accuracy; and it is in this connection that the theory is most reliable, for the effects of "gas" malalignment should be more or less the same as t_b, σ, or p are varied.

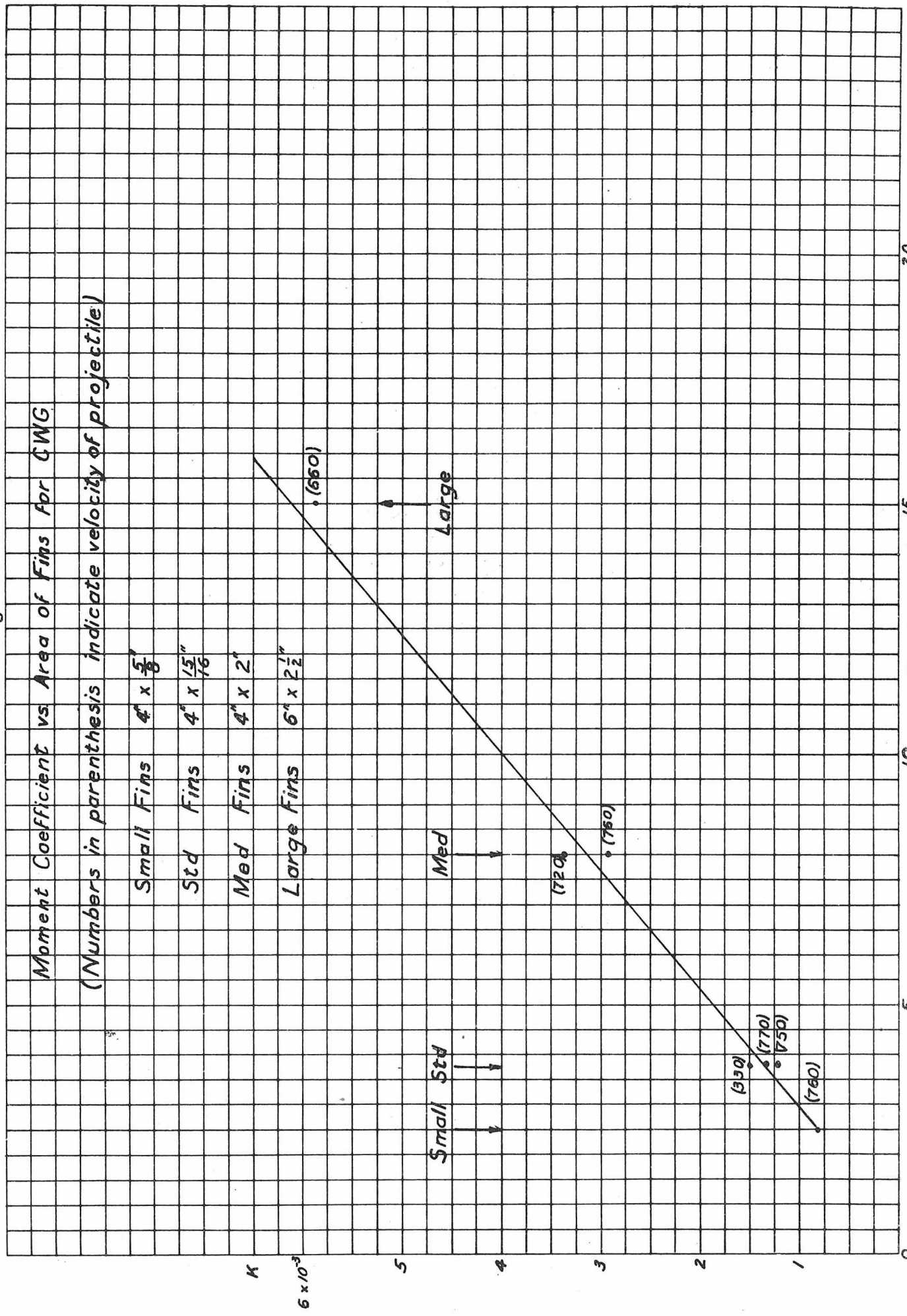
Moment Coefficient vs Area of Fins for CWG
(Numbers in parenthesis indicate velocity of projectile)
Small Fins 4" x 5/8"
Std Fins 4" x 15/16"
Med Fins 4" x 2"
Large Fins 6" x 2 1/2"
K
6 x 10^-3
5
4
3
2
1
0
5
10
15
20
Fin Area (in.^2)
Small Std
Med
Large
(660)
(720)
(760)
(760)
(750)
(770)
(730)

Fig. 10

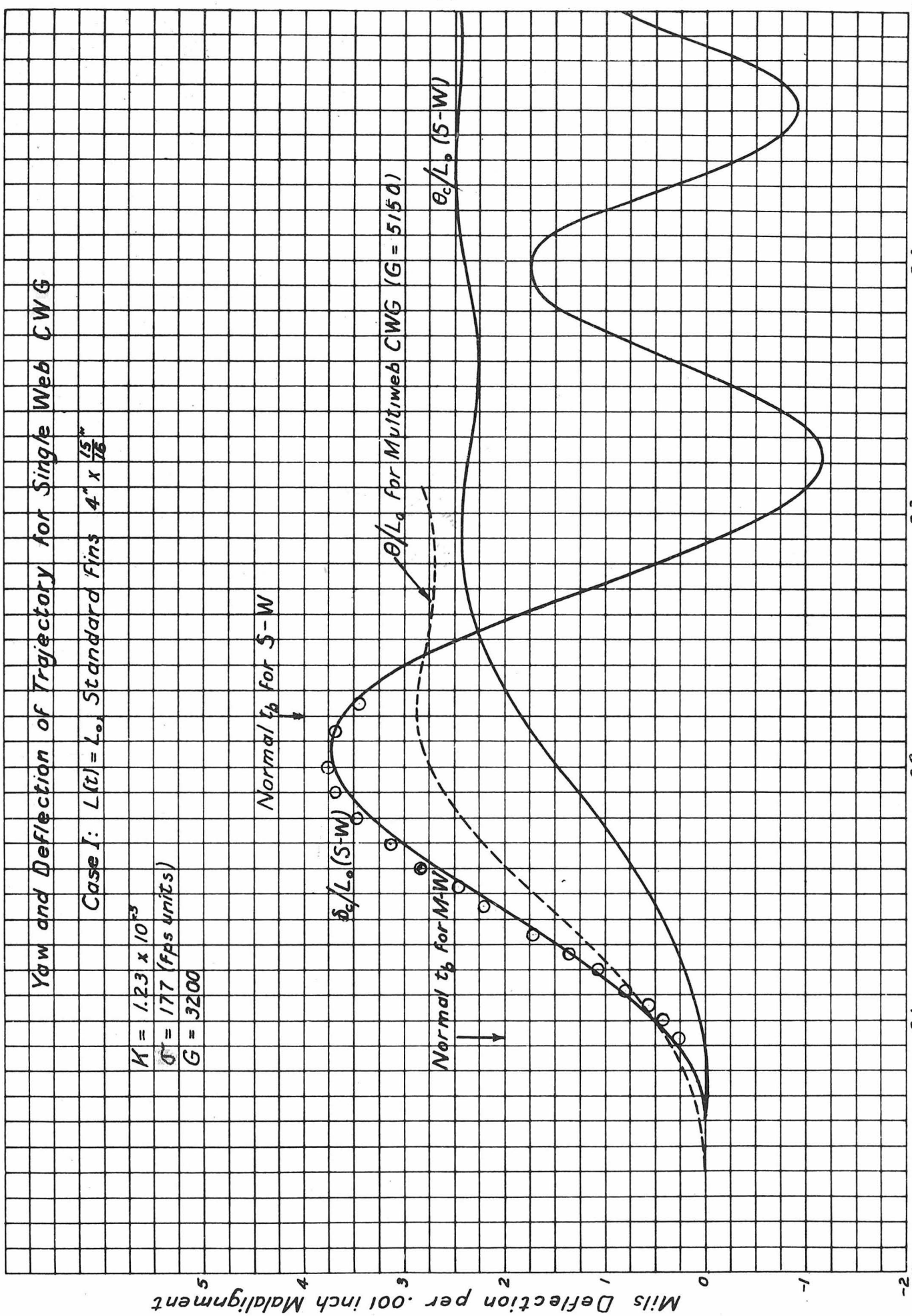
Yaw and Deflection of Trajectory for Single Web CWG
Case I: L(t) = L₀, Standard Fins 4" x 15/16"
K = 1.23 x 10⁻³
σ = 177 (fps units)
G = 3200
Normal t_b for S-W
θ/L_a for Multiweb CWG (G = 5154)
δ_c/L_a (S-W)
θ_c/L_a (S-W)
Normal t_b for M-W
Mils Deflection per .001 inch Misalignment
t (sec)
0
0.1
0.2
0.3
0.4
0.5
-2
-1
0
1
2
3
4
5

Fig. 11

Fig. 12

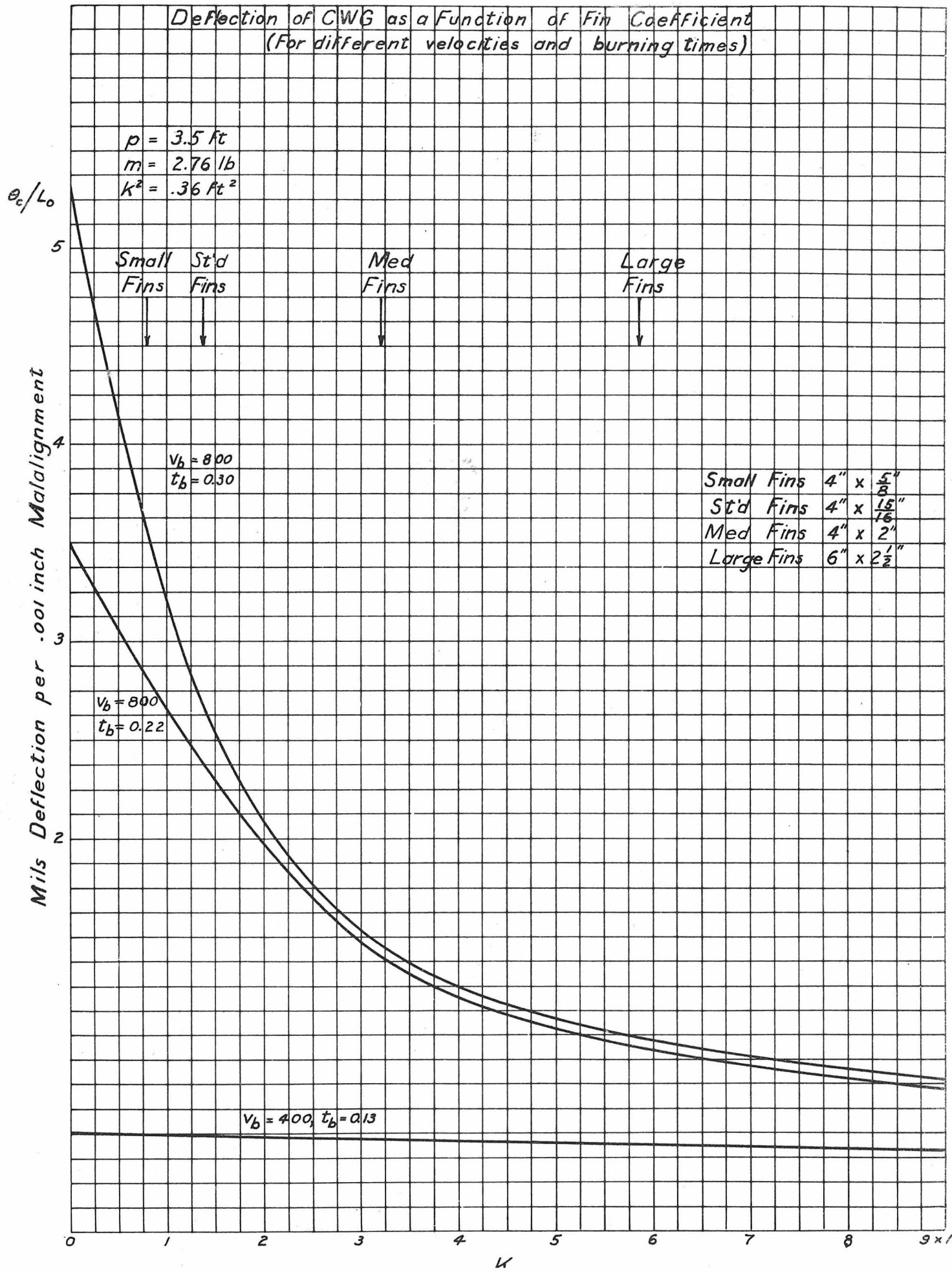
Deflection of CWG as a Function of Fin Coefficient
(For different velocities and burning times)
p = 3.5 ft
m = 2.76 lb
K² = .36 ft²
θc/Lo
Small Fins
Std Fins
Med Fins
Large Fins
Vb = 800
tb = 0.30
Vb = 800
tb = 0.22
Vb = 400, tb = 0.13
Small Fins 4" x 5/8"
Std Fins 4" x 15/16"
Med Fins 4" x 2"
Large Fins 6" x 2 1/2"
Mils Deflection per .001 inch Malalignment
5
4
3
2
0
1
2
3
4
5
6
7
8
9 x 10⁻⁷
K

Fig. 13

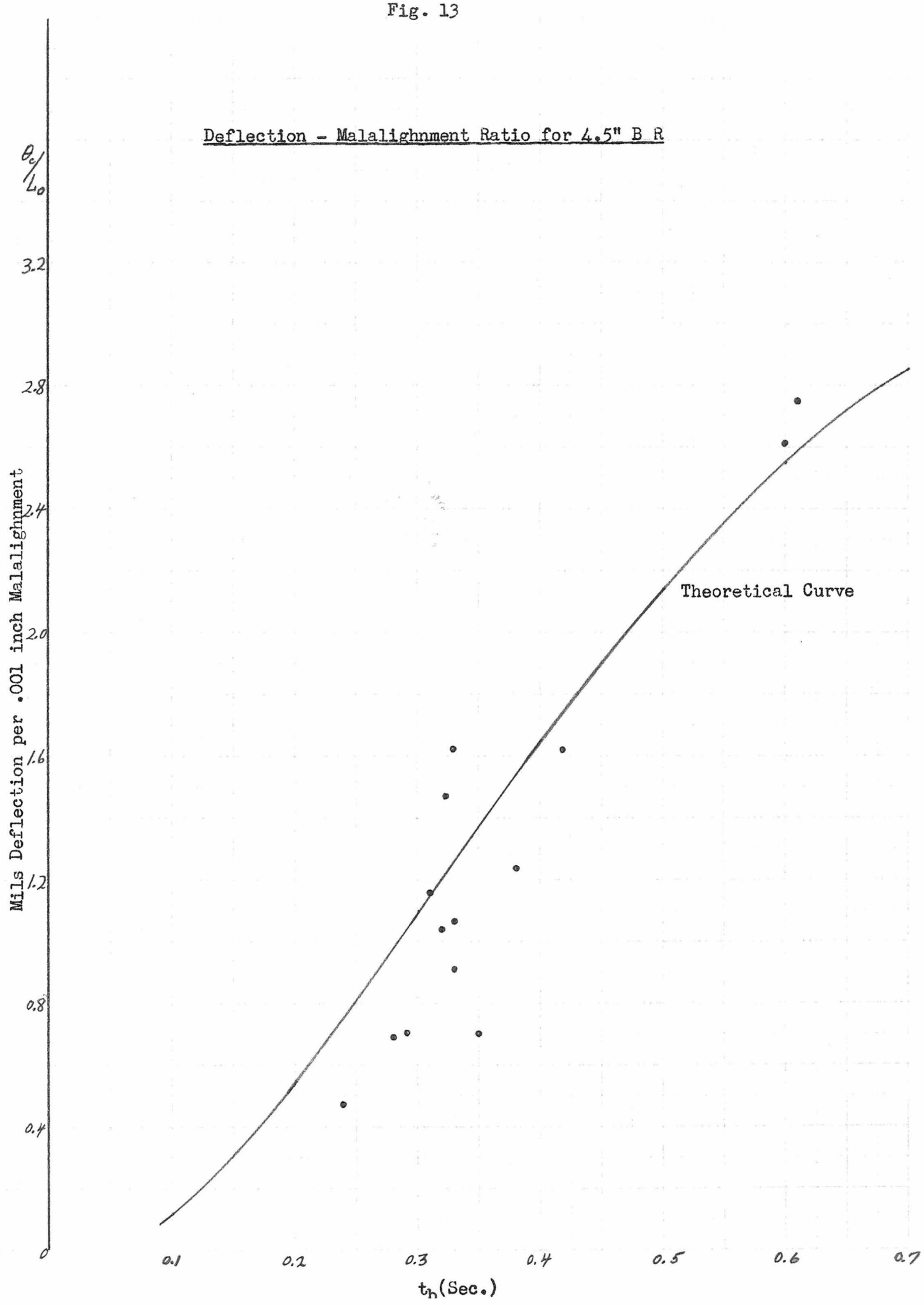
Deflection - Malalighnment Ratio for 4.5" B R
θ_c / L_o
3.2
2.8
2.4
2.0
1.6
1.2
0.8
0.4
0
Mils Deflection per .001 inch Malalighnment
Theoretical Curve
0.1
0.2
0.3
0.4
0.5
0.6
0.7
t_h(Sec.)

Fig. 14

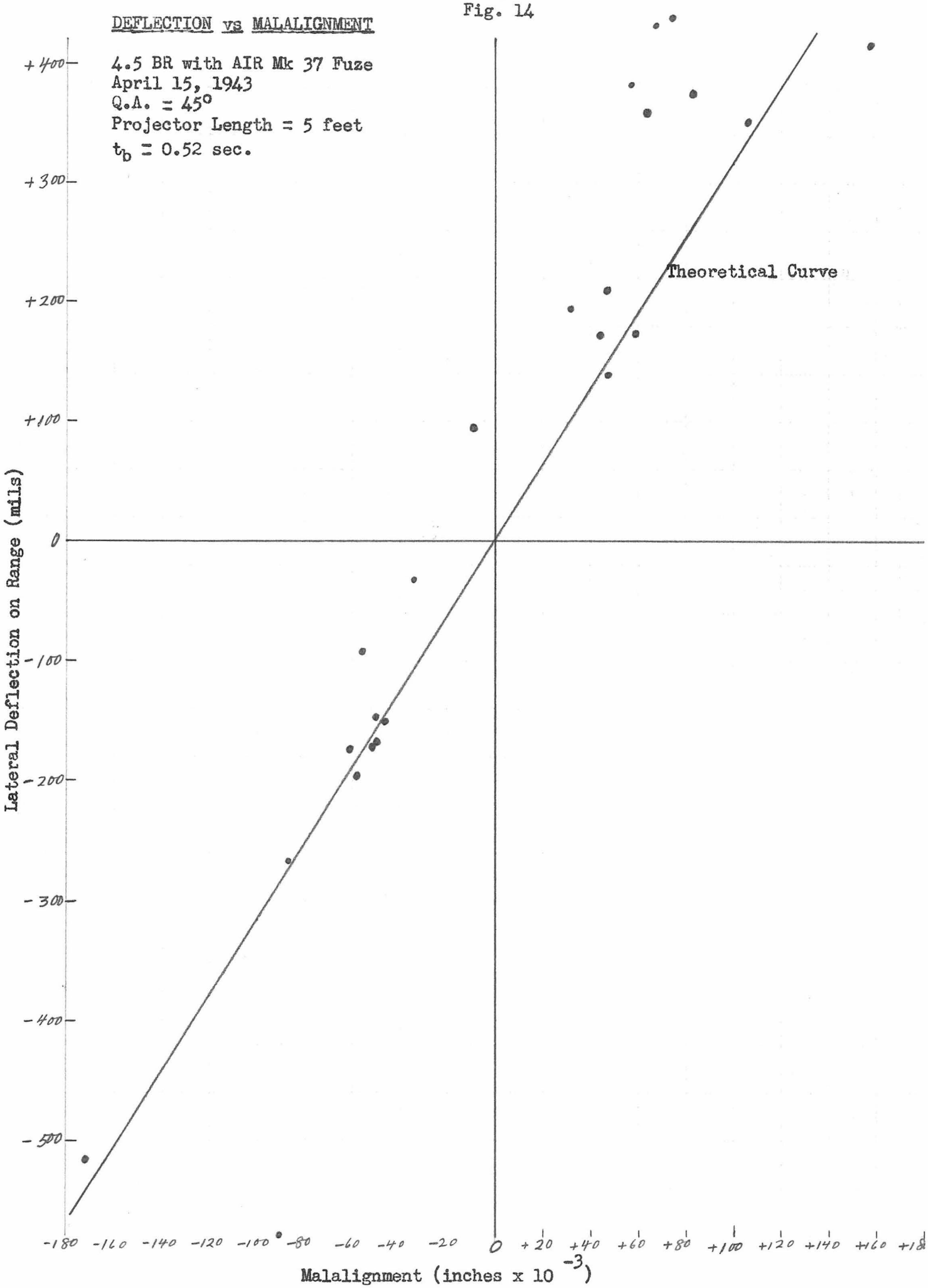
DEFLECTION vs MALALIGNMENT
4.5 BR with AIR Mk 37 Fuze
April 15, 1943
Q.A. = 45°
Projector Length = 5 feet
t_b = 0.52 sec.
Theoretical Curve
Lateral Deflection on Range (mils)
+400
+300
+200
+100
0
-100
-200
-300
-400
-500
-180 -160 -140 -120 -100 -80 -60 -40 -20 0 +20 +40 +60 +80 +100 +120 +140 +160 +180
Malalignment (inches x 10^{-3})

IV. Effect of Wind on the Mean Deflection of Rockets

A. Introduction:

In calculating the dispersion of rockets in range or in deflection for any set of firings, one should correct for the deflection of the mean of the pattern due to the influence of the wind on the motion of the projectiles. The purpose of this report is to develop formulas applicable to rockets with velocities up to about 800 ft/sec.*

The effects of wind on the motion of a rocket can be resolved into two parts: (i) effects during burning, and (ii) effects after burning.

(i) During the burning period the action of the wind on the fins will tend to turn the nose of the rocket into the wind, thus altering the direction of thrust of the motor from its initial direction on the rails. This rotation of the thrust axis will result in the deflection of the projectile into the wind, which will continue throughout the burning period.

(ii) During the post-burning period the rocket will be displaced down-wind, that is, in the direction the wind is blowing. The down-wind drift of the rocket is not due to the action of the cross-wind force on the projectile, but rather to the action of the down-wind component of the drag. The reason for this is that the period of oscillation of the projectile is small compared to the total time of flight, and since the yaw oscillations are about the position in which the yaw and cross-wind force are zero, the average cross-wind force is zero.**

---

* Leverett Davis, Jr.,[10] in CIT/MTC 6 has already developed formulas based upon assumptions which are sufficiently valid for low-velocity projectiles. His procedure is here followed in setting up the coordinate systems and the initial equations of motion.

** Strictly speaking, this is not so, since the yaw will be slowly damped out. The positive and negative cross-wind forces will thus not be equal and the average will not be zero.[11]

B. Effect of Wind during Burning:

We assume a sufficient number of rounds so that the average deflection due to malalignment and other random effects is zero. Therefore we neglect the malalignment in discussing the deflection of the "average" rocket. Also, we consider the same aerodynamic force system acting on the yawing projectile as was done in Ch. III. If we neglect the effects of gravity, drag and cross-wind force during burning, and assume that the restoring torque of the fins is proportional to the square of the velocity and to the first power of the yaw, the equation for the rotation of the rocket is

$$\ddot{\phi} = \frac{-4\pi^2}{\sigma^2} \, v_a^2 \, \delta_a \qquad (38)$$

where (See Figs. 15 and 16)

$\bar{v}_a$ = vector velocity of the rocket relative to the moving air (wind),

and δ_a = angle of yaw of the rocket with respect to the air velocity $\bar{v}_a$.

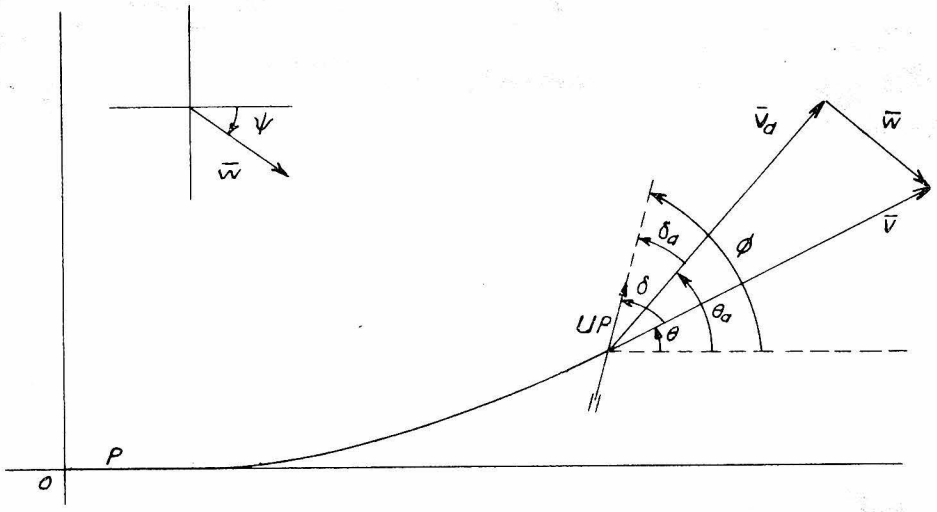

Fig. 15. Motion of Rocket in Plane of Yaw

Since we have neglected gravitational effects during burning, the motion is in the plane determined by the projector and the wind velocity vector $\bar{w}$; that is, the plane of Fig. 15. If $\bar{v}$ be the vector velocity of the projectile relative to the ground, and ψ the angle between the direction of the wind and the projector, then from Fig. 15 we get the following relations between velocities and angles:

$$v_a^2 = v^2 + w^2 - 2vw \cos (\psi + \theta)$$

$$\delta_a = \delta - (\theta_a - \theta)$$

$$\frac{w}{\sin (\theta_a - \theta)} = \frac{v_a}{\sin (\psi + \theta)}$$

Assuming that $(w/v)^2 \ll 1$, and that θ, θ_a, δ , $\delta_a \ll \pi$, we reduce the above to the approximate expressions

$$v_a = v \left(1 - \frac{w}{v} \cos \psi \right)$$

$$\theta_a - \theta = \frac{w}{v_a} \sin \psi$$

$$\delta_a = \delta - \frac{w}{v_a} \sin \psi = \delta - \frac{w}{v} \sin \psi \left(1 + \frac{w}{v} \cos \psi \right).$$

Substituting in (38) for v_a and δ_a, and again neglecting second-order terms, we get

$$\ddot{\beta} = \frac{4\pi^2}{\sigma^2} wv \sin \psi \left(1 - \frac{w}{v} \cos \psi \right) - \frac{4\pi^2}{\sigma^2} v^2 \delta \quad (39)$$

In (39) we neglect, further, the term $(w/v) \cos \psi$ compared to unity. As will be seen later, $(w/v) \cos \psi$ represents a small correction to the first term which depends upon the down-range component of $\bar{w}$, and which, for practical purposes, is negligible.

Writing Gt for v in (39), and letting

$$L_o' = \frac{4\pi^2}{\sigma^2} k^2 t_b w \sin\psi ,$$

we have

$$\ddot{\phi} = \frac{G}{k^2} \frac{L_o'}{t_b} t - \frac{4\pi^2}{\sigma^2} G^2 t^2 \delta . \qquad (40)$$

Now equating the centrifugal force on the projectile to the component of the jet force perpendicular to the trajectory, we have

$$v \dot{\theta} = G \delta ; \qquad (41)$$

and, from Fig. 1, $$\phi = \theta + \delta . \qquad (42)$$

It will be noted that Equations (40), (41) and (42) are identical with Equations (30), (31) and (32), Case II, of Ch. III. As applied to the present problem the solutions may be written as

$$\delta = \sqrt{\frac{2\pi t_b}{\sigma v_b}} w \sin\psi \cdot \Delta$$

$$\phi = \sqrt{\frac{2\pi t_b}{\sigma v_b}} w \sin\psi \cdot \Phi$$

$$\theta = \phi - \delta = \sqrt{\frac{2\pi t_b}{\sigma v_b}} w \sin\psi \cdot \Theta \qquad (43)$$

where

$$\Delta = \frac{1}{z} (1 + B_1 \delta_1 + B_2 \delta_2)$$

$$\Phi = B_1 \phi_1 + B_2 \phi_2 + B_3$$

$$\Theta = \Phi - \Delta \qquad (44)$$

$$z = \sqrt{\frac{2\pi G}{\sigma}} t ,$$

and δ_1, δ_2, ϕ_1, ϕ_2, B_1, B_2 and B_3 are given by equations (33) and (35).

The value of θ at the end of burning ($t = t_b$) is then the deflection of the trajectory in the plane of yaw from the initial direction, and, from

Eq. (41) is the final direction of flight of the rocket. (The effect of wind after burning will be discussed later.) In order to determine what lateral and vertical deflections on range the above leads to, consider Fig. 16.

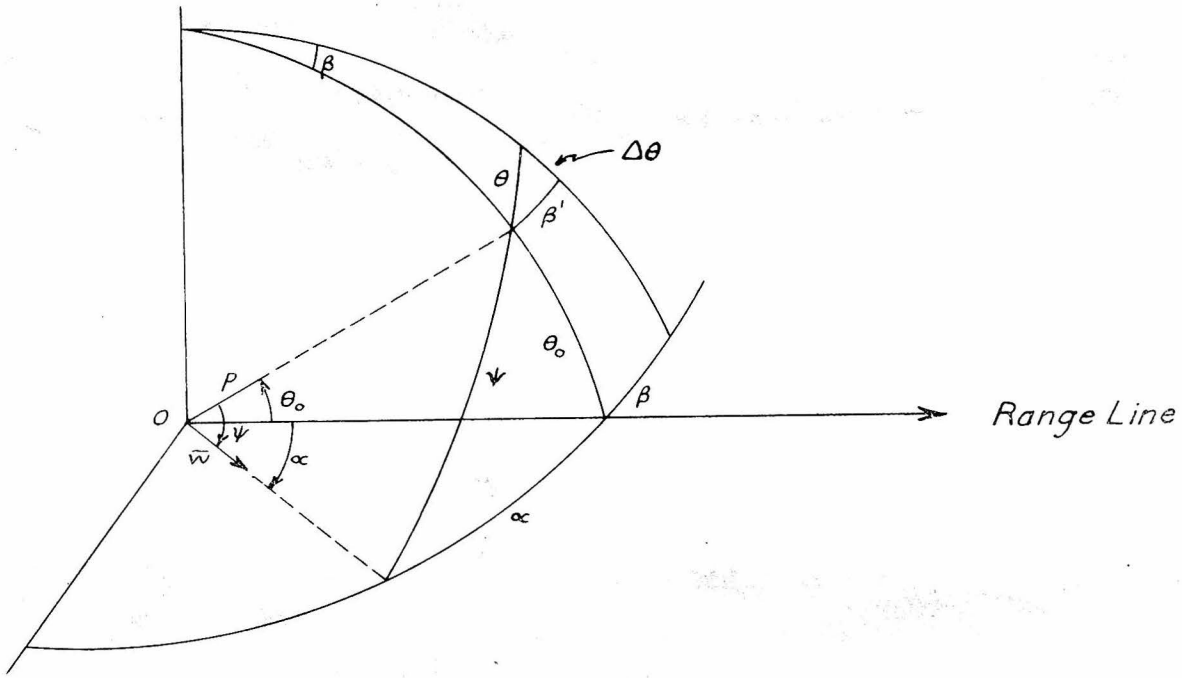

Fig. 16. Deflection of Rocket

If $\Delta\theta_0$ is the increase in departure angle at end of burning and β_0 is the lateral deflection of the plane of the trajectory, it can be easily demonstrated that

$$\beta_0 = \frac{\theta \sin \alpha}{\cos \theta_0 \sin \psi}$$

and

$$\Delta\theta_0 = \theta \frac{\sin \theta_0 \cos \alpha}{\sin \psi}$$

where α is the angle between the range line and the direction in which the wind is blowing, measured clockwise from the range line. Letting

$W_\perp = w \sin \alpha$ = cross-range component of wind velocity,

$W_{//} = w \cos \alpha$ = down-range component of wind velocity,

and substituting for θ from equation (43), we have finally

$$\beta_o/W_\perp = \sqrt{\frac{2\pi t_b}{\sigma v_b}} \cdot \frac{\omega}{\cos \theta_o} \qquad (45)$$

$$\Delta\theta_o/W_{\parallel} = \sqrt{\frac{2\pi t_b}{\sigma v_b}} \cdot \sin \theta_o \cdot \omega \qquad (46)$$

where ω is given by (44).

Eqs. (45) and (46) give the deflections produced by the wind during the burning period of the rocket. In Fig. 17 are plotted the solutions of Equations (45) and (46) which give values of $(\beta_o/W_\perp)\, v_b \cos \theta_o$ as a function of $\frac{v_b t_b}{\sigma}$ for several values of p/σ. By the use of these curves one can get values of $\beta_o/W_\perp$ for any desired combination of values of v_b, t_b, σ, p and θ_o. One can also derive the values of $\Delta\theta_o/W_{\parallel}$, for $(\Delta\theta_o/W_{\parallel}) = (\beta_o/W_\perp) \sin \theta_o \cos \theta_o$.

C. Effect of Wind after Burning:

For the purpose of calculating the down-wind drift of the rocket we shall assume that the effects of cross-wind due to yaw average out to zero during the flight, as mentioned previously. Also, since we are interested here only in the lateral deflection, we consider only the cross-range component $W_\perp$ of the wind, since the sole effect of $W_{\parallel}$ is to modify the range. The drag, however, acts in the negative direction of the velocity of the projectile relative to the air ($-\bar{v}_a = -\bar{v} + \bar{w}$); consequently, there is always a component of drag in the direction of the wind $\bar{w}$. By considering the motion of the projectile relative to a coordinate system moving with the air, the problem can be treated in the same manner as the wind deflection for shells.[12] Consider two systems of coordinates, one moving with the velocity of the air and the other fixed relative to the ground, with the x-axis pointing along the range and with both systems coinciding at the end of burning at the point where the rocket begins its post-burning flight.

Fig. 17

MEAN WIND DEFLECTION DURING BURNING

β = Deflection of trajectory into the wind (mils)
$w_\perp$ = Cross-range component of wind velocity (ft/sec)
v_b = Velocity of rocket at end of burning (ft/sec)
t_b = Time at which burning ceases (sec)
σ = Wave-length of yaw oscillation (ft)
p = Effective projector length (ft)
θ = Quadrant angle of projector

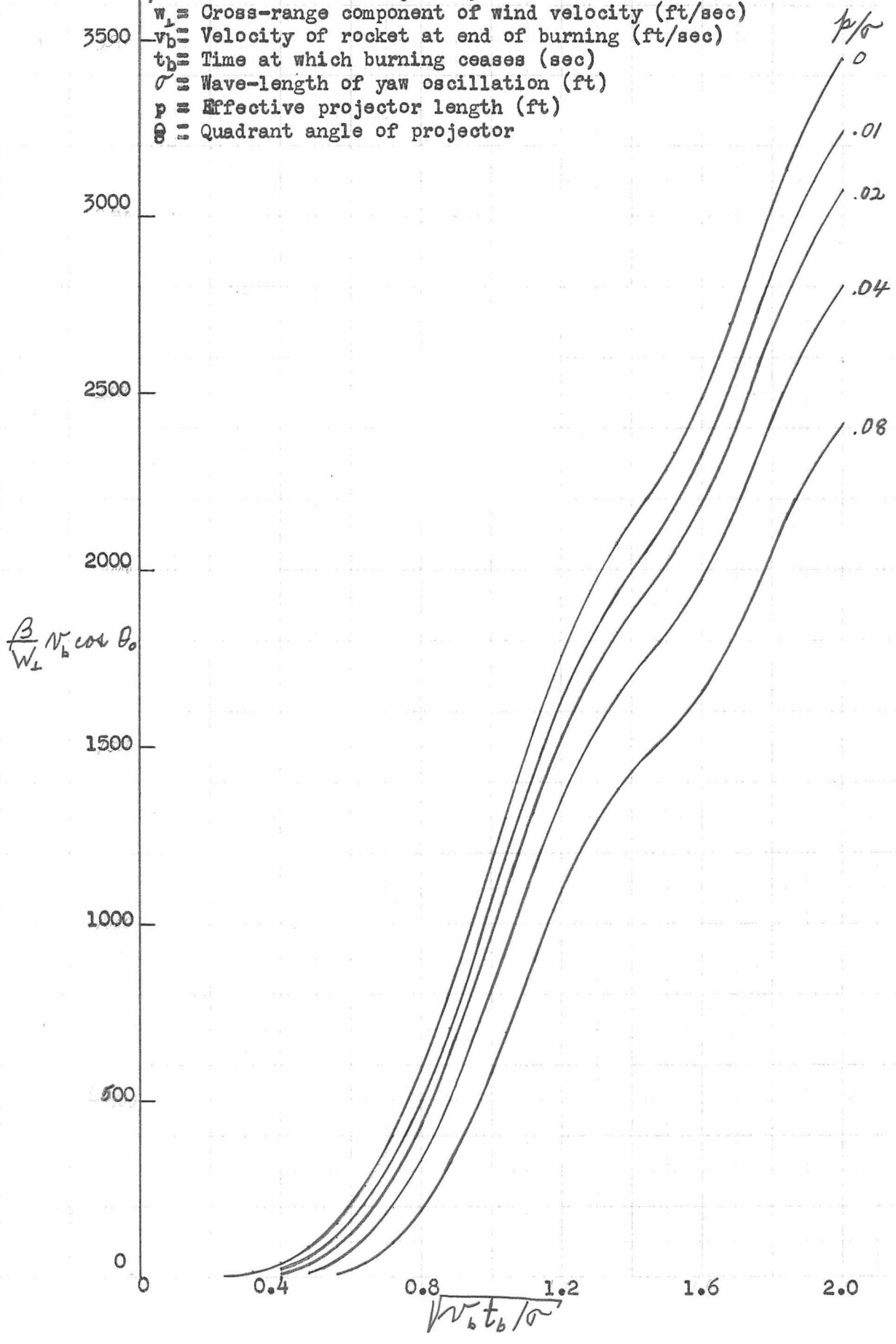

If γ be the angle between the plane of the trajectory relative to the moving coordinates and the plane of the trajectory relative to the fixed coordinates, it is very nearly equal to

$$\gamma = \frac{W_\perp}{v_b \cdot \cos \theta_b}$$

Therefore, in the range X the total lateral deviation of the shell relative to the air is $-\frac{W_\perp X}{v_b \cos \theta_b}$. However, in the time of flight T_1 the moving origin has moved through the distance $W_\perp T_1$. Thus the net linear drift during the flight is

$$W_\perp T_1 - \frac{W_\perp X}{v_b \cos \theta_b} ,$$

and the total angular down-wind drift of the projectile is

$$\beta_1 / W_\perp = \frac{1}{X} \left[T_1 - \frac{X}{v_b \cos \theta_b} \right] . \qquad (47)$$

For T_1 we shall use the Didion-Bernoulli expression (See Eq. (16), Ch. II).

$$T_1 = \frac{X}{v_b \cos \theta_b} D(Z)$$

where $$D(Z) = \frac{e^{Z/2} - 1}{Z/2} .$$

In this expression, $Z = 2c \alpha X$, where

c = deceleration coefficient of the projectile,

and α = average of $1/\cos \theta$ in the Didion-Bernoulli method.

Thus, for the final form of the angular down-wind drift we may write

$$\beta_1 / W_\perp = \frac{1}{v_b \cos \theta_b} \left[D(Z) - 1 \right] . \qquad (48)$$

D. Limitations of Theory:

1. In setting up the above equations we assumed that $(w/v)^2$ is negligible compared to unity. We shall examine this for three rockets having

different velocities. In Table 5 are given the values of $(w/v)^2$ at $v = v_p$ (the velocity of the rocket as it leaves the rails), at $v = v_b$ (the burnt velocity), and also the average value of $(w/v)^2$ during the burning period. In all of the cases, w = 15 mph = 22 ft/sec. Except for the ASPC, the errors introduced by neglecting $(w/v)^2$ are quite negligible. Of course, as the wind velocity increases the error increases as w^2.

Table 5

UP	v_b (ft/sec)	t_b (sec)	v_p (ft/sec)	$(w/v_p)^2$	$(w/v_b)^2$	$(w/v)^2_{av}$
ASPC	170	.35	66	.111	.016	.042
4.5 BR	360	.35	85	.067	.0037	.016
CWB	720	.50	152	.021	.0009	.0044

2. A far more serious error was introduced by neglecting $(w/v) \cos \gamma$ compared to unity in Eq. (39). Now (see Fig. 16)

$$\cos \gamma = \cos \alpha \cos \theta_o$$

$$\therefore \quad (w/v) \cos \gamma = (W_{\prime\prime}/v) \cos \theta_o$$

Let us investigate the validity of this assumption for the ASPC, 4.5 BR, and CWB. For a down range component of wind, $W_{\prime\prime}$, equal to 15 mph (22 ft/sec), table 6 gives the values of $(W_{\prime\prime}/v) \cos \theta_o$ at the instant the rocket leaves the rails and at the time burning ceases, as well as the average value during the burning period. In general, the accuracy does not warrant taking this effect into account. But if such is not the case, one can get a rough approximation to the correct result by modifying equations (45) and (46) to read

$$\beta_o/W_\perp = \sqrt{\frac{2\pi t_b}{\sigma v_b}} \frac{1}{\cos \theta_o} \left[1 - (W_{\parallel}/v)_{av} \cos \theta_o \right] \cdot \textcircled{\sim} \qquad (45a)$$

$$\Delta\theta_o/W_{\parallel} = \sqrt{\frac{2\pi t_b}{\sigma v_b}} \sin \theta_o \left[1 - (W_{\parallel}/v)_{av} \cos \theta_o \right] \cdot \textcircled{\sim} \qquad (46a)$$

Table 6

UP	θ_o	v_b	v_p	$(W_{\parallel}/v_p)\cos\theta_o$	$(W_{\parallel}/v_b)\cos\theta_o$	$(W_{\parallel}/v)_{av}\cos\theta_o$
ASB	45°	170	66	.24	.091	.14
4.5 BR	45°	360	85	.18	.045	.082
CWB	45°	720	152	.10	.022	.043

3. It has been assumed throughout that the aerodynamic forces on the projectile follow the v^2 law. Since the v^2 law is valid only up to velocities of 800 ft/sec, the above equations are valid only under the same restriction. Also, it has been assumed that the wind is constant for all the rounds of a set and that it is not a function of altitude.

4. It must be remembered, too, that the above equations apply to the mean deflection of a given set of firings only when a sufficient number of rounds have been fired so that malalignment and other random effects average out.

E. Observational Data:

Since most range firing tests have been made with little or no wind prevailing, very little experimental data for comparison with theory is available. In the accompanying plot are shown the observed and predicted mean deflections for the ASB for a number of tests (Data from CIT/IBC 10). Though very few rounds make up the means, there seems to be a general

qualitative agreement between the observed and predicted deflections. One would expect low temperature (i.e., long burning time) rounds to be deflected up-wind, since then the effect during burning is greatest. On the other hand, at high temperatures (i.e., short burning time) one would expect the rockets to be deflected down-wind, since then the effect during burning is slight compared to the down-wind drift during free flight. This is borne out in a general way by the above data, for the mean of all tests gives the following (negative values correspond to deflections up-wind):

Temperature	Mean Deflections (all winds)
0° F	- 8.0 mils
70° F	+ 0.4 mils
125° F	+ 5.5 mils

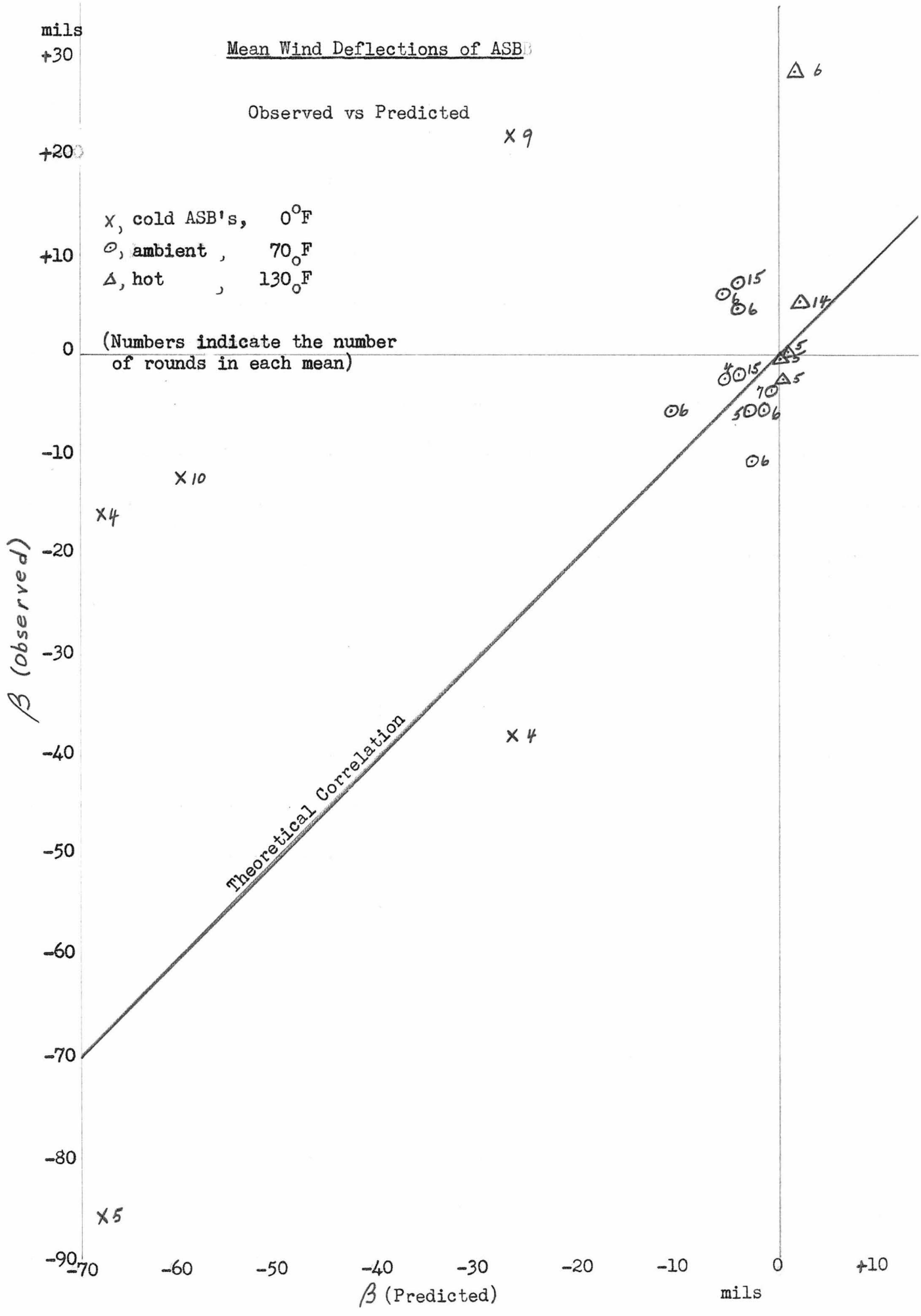
mils
Mean Wind Deflections of ASB
Observed vs Predicted
X, cold ASB's, 0°F
⊙, ambient , 70°F
Δ, hot , 130°F
(Numbers indicate the number of rounds in each mean)
Theoretical Correlation
β (observed)
β (Predicted)
mils
+30
+20
+10
0
-10
-20
-30
-40
-50
-60
-70
-80
-90
-70
-60
-50
-40
-30
-20
-10
0
+10
X 9
X 10
X 4
X 4
X 5
Δ 6
⊙ 15
⊙ 6
Δ 14
⊙ 6
Δ 5
Δ 5
⊙ 4
⊙ 15
Δ 5
⊙ 7
⊙ 6
⊙ 5
⊙ 6
⊙ 6

Appendix 1. Studies of "Gas" Malalignment by Means of the Yaw Machine (CIT/PMC 1.39)

In order to learn something about the nature of the so-called "gas" malalignment and its effect upon accuracy of rockets, Prof. Bowen had built a "yaw machine" (See CIT/PMC 1.39.) by means of which it is possible to measure the angular acceleration of a motor during burning and determine from that the torque or the equivalent side force at the nozzle which produced this acceleration. Since the instrument gives a record only of the side force as a function of time it is necessary to interpret the data in such a way as to predict its performance in actual flight. For expressing the performance of a given motor in terms of freedom from yaw and deflection in flight the following index of dispersion has been adopted.

If a projectile without fins experiences an angular impulse $L\Delta t$ at time t_1, the UP will rotate with angular velocity $\dot{\phi}$ given by (See Fig. 5.)

$$I\dot{\phi} = L\Delta t \qquad (1)$$

where I is the moment of inertia of the UP about its center of gravity. The equations of motion of the UP from then on are:

$$\ddot{x} = G\cos\phi \simeq G \qquad (2)$$

$$\ddot{y} = G\sin\phi \simeq G\phi \qquad (3)$$

Integrating (1),

$$\phi = \frac{L\Delta t}{I}(t - t_1) \qquad (4)$$

Substituting into (3) and integrating,

$$\dot{y} = \frac{GL\Delta t}{2I}(t - t_1)^2 \qquad (5)$$

From (2),

$$\dot{x} = G\,t$$

Thus the deflection of the trajectory at any time $t > t_1$ is given by

$$\theta \cong \tan \theta = \frac{\dot{y}}{\dot{x}} = \frac{L \Delta t}{2I} \frac{(t - t_1)^2}{t} \qquad (6)$$

and at the end of burning, $t = t_b$,

$$\Delta \theta_b = \frac{L \Delta t}{2I} \frac{(t_b - t_1)^2}{t_b} . \qquad (7)$$

We have then that the deflection to be expected due to a given impulse $L \Delta t$ at time t is proportional to $\frac{(t_b - t)^2}{t_b}$, which we call the weighting factor for each value of the side force (which is proportional to the impulse) as registered by the yaw machine. The integrated deflection for any motor is then

$$\theta_b = \sum_{t=t_p}^{t=t_b} \frac{L \Delta t}{2I} \frac{(t_b - t)^2}{t_b} = \int_{t_p}^{t_b} \frac{L}{2I} \frac{(t_b - t)^2}{t_b} dt, \qquad (8)$$

where t_p is the time the UP leaves the projector and t_b is the time at which burning ceases.

We can replace the torque L by F_s l where F_s is the side force acting at a distance l from the center of gravity. The quantity

$$\sum_{t=t_p}^{t=t_b} \frac{F_s (t_b - t)^2}{t_b} \Delta t$$

is called the index of dispersion, which is a measure of the dispersion to be expected from a rocket with no fins.

The weighting factor due to fin action would tend to reduce the "ID". However, this weighting factor involves complicated integrals and so will not be included here. In any case, the effect of fins would be more or less the same on each UP. Thus on a relative scale, the index of dispersion should be a rather good measure of the relative dispersions to be expected on the range from various motors with different nozzles.

One such curve of F_s as a function of time is shown in Fig. 18. The striking feature is the reversal in the side force, which represents a violent change in the direction of the malalignment. This phenomenon is what has been associated with the term "gas" malalignment, and its presence can now no longer be doubted. One gets rid of the mechanical (or geometrical) malalignment in the computations by taking the average value of the index of dispersion from the mean of a number of similar tests with the same motor and nozzle.

If the constants of the CWG are substituted into equation (8), it is found that the deflections due to the random "gas" malalignment are of the order of two to three times the deflections due to 0.010 inch mechanical malalignment. Herein lies the explanation of the large discrepancy between the observed and predicted (on the basis of geometrical malalignment alone) deflections for this rocket. (cf. CIT/JPC 3.)

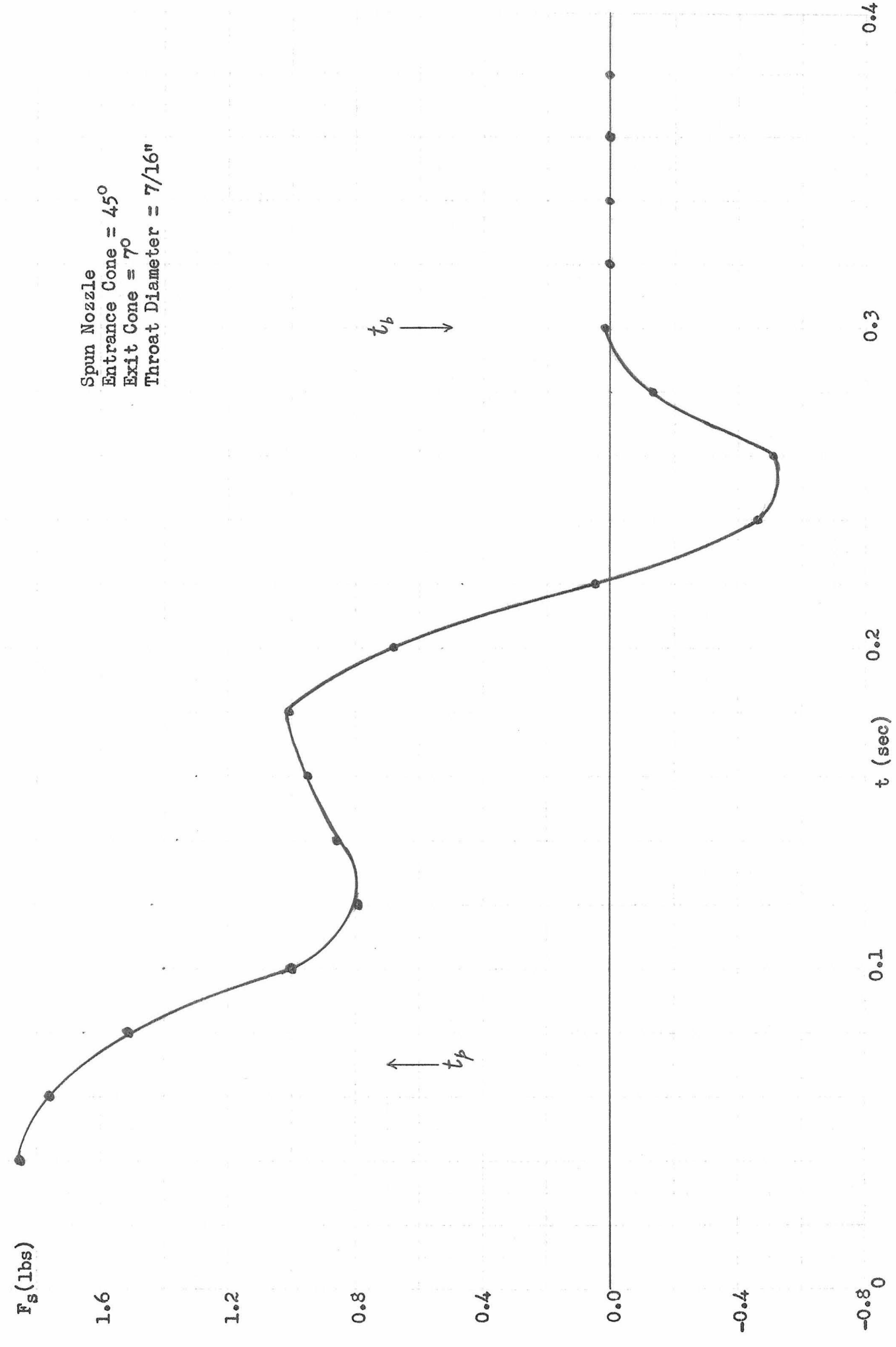

Fig. 18 -- Side Force at the Nozzle

Appendix 2. Method of Solution of Equations for Yaw and Deflection*

The equations of motion of a rocket during the burning period were given in Ch. III as

$$\ddot{\phi}_c = \frac{G\,L(t)}{k^2} - \frac{4\pi^2 G^2 t^2\, \delta_c}{\sigma^2} \tag{30}$$

$$t\,\dot{\theta}_c = \delta_c \tag{31}$$

$$\phi_c = \theta_c + \delta_c \tag{32}$$

For a malalignment of the form

$$L(t) = At - B \tag{33}'$$

The method of solution is briefly as follows:

Letting $$z = \sqrt{\frac{2\pi G}{\sigma}}\, t$$

and $$\left.\begin{matrix}\phi_c \\ \theta_c \\ \delta_c\end{matrix}\right\} = \frac{\sigma A}{2\pi k^2} \sqrt{\frac{\sigma}{2\pi G}} \left\{\begin{matrix}\Phi \\ \Theta \\ \Delta\end{matrix}\right.$$

equations (30), (31), (32) become

$$\Phi'' = -\frac{B}{A}\sqrt{\frac{2\pi G}{\sigma}} + z - z^2\Delta$$

$$z\Theta' = \Delta$$

and $$\Phi = \Theta + \Delta,$$

where the primes indicate differentiation with respect to z. From these one obtains without difficulty the following equations in Φ and Δ.

---

* Method of L. Davis, Jr.

$$z\,\Phi''' - \Phi'' + z^3\Phi' = K$$

$$z^2\Delta'' + z\,\Delta' - (1 - z^4)\Delta = -K\,z^2 + z^3$$

where $K = \frac{B}{A}\sqrt{\frac{2\pi G}{\sigma}}$.

Solution of Φ equation

$$z\,\Phi''' - \Phi'' + z^3\Phi' = K$$

In terms of $y = \Phi'$,

this becomes $zy'' - y' + z^3 y = K$.

Assuming a series solution of the form

$$y = \sum b_n z^n \quad ,$$

we find that

$$y = \Phi' = b_1 \sum_{n=0}^{\infty} (-1)^n \frac{(z^2/2)^{2n}}{(2n)!} + b_2 \sum_{n=0}^{\infty} (-1)^n \frac{(z^2/2)^{2n+1}}{(2n+1)!} - K\left(z - \frac{z^5}{3\cdot5} - \frac{z^9}{3\cdot5\cdot7\cdot9} - \cdots\right)$$

or, $$\Phi' = b_1 \cos z^2/2 + b_2 \sin z^2/2 - K\left(z - \frac{z^5}{3\cdot5} - \frac{z^9}{3\cdot5\cdot7\cdot9} - \cdots\right) .$$

Integrating,

$$\Phi = b_1\sqrt{\pi}\,C(z/\sqrt{\pi}) + b_2\sqrt{\pi}\,S(z/\sqrt{\pi}) - K\sum_{n=0}^{\infty} \frac{(-1)^n z^{4n+2}}{1\cdot3\cdot5\cdots(4n+1)(4n+2)} + b_3$$

where

$$C(z/\sqrt{\pi}) = \frac{1}{\sqrt{\pi}}\int_0^z \cos\frac{x^2}{2}\,dx = \int_0^u \cos\frac{\pi u^2}{2}\,du = C(u)$$

and

$$S(z/\sqrt{\pi}) = \frac{1}{\sqrt{\pi}}\int_0^z \sin\frac{x^2}{2}\,dx = \int_0^u \sin\frac{\pi u^2}{2}\,du = S(u)$$

are the Fresnel integrals familiar in optical diffraction theory. Dr. Morgan Ward, has shown that it is also possible to express the third term in the above solution for Φ in terms of the Fresnel integrals, namely

$$\sum_{n=0}^{\infty} \frac{(-1)^n \, z^{4n+2}}{1\cdot3\cdot5\cdots(4n+1)(4n+2)} = \frac{\pi}{2}\left\{ S^2(z/\sqrt{\pi}) + C^2(z/\sqrt{\pi}) \right\} .$$

The complete solution for Φ is then

$$\Phi = b_1\sqrt{\pi}\, C(z/\sqrt{\pi}) + b_2\sqrt{\pi}\, S(z/\sqrt{\pi}) - \frac{\pi}{2} K\left\{ S^2(z/\sqrt{\pi}) + C^2(z/\sqrt{\pi}) \right\} + b_3 .$$

Solution of Δ equation

$$z^2\,\Delta'' + z\,\Delta' - (1-z^4)\,\Delta = -K\,z^2 + z^3$$

Again assuming a series solution of the form

$$\Delta = \sum a_n \, z^n$$

we find

$$\Delta = \frac{a_1}{z}\sum_{n=0}^{\infty} \frac{(-1)^n (z^2/2)^{2n}}{(2n)!} + \frac{a_2}{z}\sum_{n=0}^{\infty} \frac{(-1)^n (z^2/2)^{2n+1}}{(2n+1)!} + \frac{1}{z} - \frac{K}{z}\sum_{n=0}^{\infty} \frac{(-1)^n \, z^{4n+3}}{1\cdot3\cdot5\cdots(4n+3)} .$$

Leverett Davis has shown that the last term could be written as

$$\delta_o = \sum_{n=0}^{\infty} \frac{(-1)^n \, z^{4n+3}}{1\cdot3\cdot5\cdots(4n+3)} = \sin(z^2/2)\sqrt{\pi}\, C(z/\sqrt{\pi}) - \cos(z^2/2)\sqrt{\pi}\, S(z/\sqrt{\pi}) ,$$

when the complete Δ solution is

$$\Delta = \frac{1}{z}\left\{ a_1 \cos(z^2/2) + a_2 \sin(z^2/2) + 1 - K\,\delta_o \right\} .$$

The boundary conditions upon these equations is that at the time the UP leaves the projector, both the yaw and deflection and their angular velocities are zero; i.e. $\delta_c = \dot{\delta}_c = \theta_c = \dot{\theta}_c = \phi_c = \dot{\phi}_c = 0$.

Hence, at $z = z_p$, it follows that

$$\Delta = \dot{\Delta} = \Phi = \dot{\Phi} = 0 \quad .$$

Inserting these initial conditions into the solutions for Φ and Δ, and substituting back to our original variable we have finally

$$\delta_c = \frac{AG}{k^2} \left(\frac{\sigma}{2\pi G}\right)^{3/2} \frac{1}{z} \cdot \left(\alpha_1 \delta_1 + \alpha_2 \delta_2 - \frac{B}{A}\sqrt{\frac{2\pi G}{\sigma}}\,\delta_o + 1\right)$$

$$\phi_c = \frac{AG}{k^2} \left(\frac{\sigma}{2\pi G}\right)^{3/2} \left(\alpha_1 \phi_1 + \alpha_2 \phi_2 - \frac{B}{A}\sqrt{\frac{2\pi G}{\sigma}}\,\phi_o + \alpha_3\right)$$

$$\theta_c = \phi_c - \delta_c$$

where
$$\phi_1(z) = -\sqrt{\pi}\, S(z/\sqrt{\pi})$$
$$\phi_2(z) = \sqrt{\pi}\, C(z/\sqrt{\pi})$$
$$\phi_o(z) = \frac{1}{2}\left[\phi_1^2(z) + \phi_2^2(z)\right]$$
$$\delta_1(z) = \cos z^2/2$$
$$\delta_2(z) = \sin z^2/2$$
$$\delta_o(z) = \delta_1(z) \cdot \phi_1(z) + \delta_2(z) \cdot \phi_2(z)$$
$$\alpha_1 = \frac{B}{A}\sqrt{\frac{2\pi G}{\sigma}}\,\phi_1(z_p) - \delta_1(z_p)$$
$$\alpha_2 = \frac{B}{A}\sqrt{\frac{2\pi G}{\sigma}}\,\phi_2(z_p) - \delta_2(z_p)$$
$$\alpha_3 = -\frac{B}{A}\sqrt{\frac{2\pi G}{\sigma}}\,\phi_o(z_p) + \delta_o(z_p)$$

where $z_p = \sqrt{\frac{2\pi G}{\sigma}}\; t_p = \sqrt{4\pi p/\sigma}$ is the value of z when $t = t_p$.

Applications of solution

(i) For $A = L_o'/t_b$, $B = 0$,

the above equations give the solutions for Case II in Ch. III.

(ii) For $A = -L_o'/t_b$, $B = -L_o'$,

the equations give the solutions for Case III in Ch. III.

(iii) For $A = (4\pi^2/\sigma^2)\, k^2\, w \sin\varphi$, and $B = 0$,

the above results give the solutions for the wind equations in Ch. IV.

Appendix 3. Forward Firing of Rockets From Airplanes or Moving Projectors

The theory of yaw and deflection developed in Ch. III can just as well be used for predicting accuracy when the rocket is fired forward (or backward, if $v_A < v_b$) from a plane or from any vehicle which itself has an air velocity v_A. We shall consider two coordinates system: one at rest relative to the ground with the origin at the projector at the moment of fire and the other moving with the constant velocity v_A of the projector. Primed quantities will refer to the coordinate system fixed with respect to the ground and unprimed quantities to the moving system.

The air velocity of the UP is then $v' = v_A + Gt$, if the acceleration ($G = v_b/t_b$) is assumed constant, and the equations of motion become (cf Ch.III).

$$\ddot{\phi}_c = \frac{GL_0}{k^2} - \frac{4\pi^2}{\sigma^2}(v_A + Gt)^2 \delta_c$$

$$(v_A + Gt)\,\dot{\theta}_c = G\,\delta_c$$

$$\phi_c = \theta_c + \delta_c \quad .$$

In terms of the new time $t' = \frac{v_A}{G} + t$, the above equations are identical with equations (30), (31), (32); and therefore the solutions given in Ch. III are applicable in this case.

Hence, if the primed quantities

$$t_b' = \frac{v_A}{G} + t_b = \frac{v_A + v_b}{v_b}\, t_b$$

$$v_b' = v_A + G\, t_b = v_A + v_b$$

$$p' = \tfrac{1}{2} G\, t_p'^2 = \left(\sqrt{p} + v_A \sqrt{\frac{t_b}{2v_b}}\right)^2$$

are used in connection with Figs. 7, 8 and 9 (σ should be used in place of T, since σ is constant while T varies with the velocity), one gets the predicted deflection for this type of firing.

References and Notes

1) Stodola and Loewenstein, Steam and Gas Tubines, p. 1, New York, 1927.

2) "Rocket and Rocket Apparatus", Encyclopedia Brittanica, (1929).

3) Hayes, T. J., Elements of Ordnance, Ch. X, "Exterior Ballistics", New York, 1938.

4) Biot, M. A., Dynamic Stability of Bombs and Projectiles, Ch. I, "Forces on a Solid Moving Through an Ideal Fluid", CIT/JPC 4.

5) Hayes, loc. cit, Figures 224, 225, 226.

6) Cranz, C., Lehrbuch der Ballistik, Vol. I, Berlin, 1925.

7) For application of the Didion-Bernoulli approximation to rockets, see Davis, L., "Exterior Ballistics of Rockets", CIT (unpublished); and Dempster, A. J., "Rocket Targets", NDRC Report A-28.

8) Davis, L., "Yaw and Deflection of UP's", CIT/MTC 3.

9) Davis, L., "Initial Conditions for the Calculation of CWG Trajectories", CIT/MTC 2.

10) Davis, L., "Effect of Wind on the Trajectory of a UP", CIT/MTC 6.

11) Biot, loc. cit, Ch. III, "Stability of the Rectilinear Trajectory in Air and Water Neglecting Gravity", CIT/JPC 6.

12) The method used is given in the introduction to Exterior Ballistic Tables, Vol. I, Ordnance Department, U. S. Army, 1924.